International Journal of Mass Spectrometry 306 (2011) 9–26

Contents lists available at ScienceDirect

International Journal of Mass Spectrometry

journal homepage: www.elsevier.com/locate/ijms

The dissociation chemistry of low-energy *N*-formylethanolamine ions: Hydrogen-bridged radical cations as key intermediates

Karl J. Jobst[a], Richard D. Bowen[b], Johan K. Terlouw[a,*]

[a] Department of Chemistry and Chemical Biology, McMaster University, 1280 Main Street West, Hamilton, ON, L8S 4M1, Canada
[b] School of Life Sciences, University of Bradford, Richmond Road, Bradford, West Yorkshire, BD7 1DP, UK

ARTICLE INFO

Article history:
Received 19 April 2011
Received in revised form 17 May 2011
Accepted 17 May 2011
Available online 26 May 2011

In memory of Professor Dudley H. Williams, whose pioneering studies on the role of ion–neutral complexes in gas-phase ion chemistry have set the stage for this contribution.

Keywords:
Tandem mass spectrometry
CBS-QB3 model chemistry
C_3H_5NO ion structures
Conformers
Quid-pro-quo catalysis

ABSTRACT

Tandem mass spectrometry experiments show that *N*-formylethanolamine molecular ions $HOCH_2CH_2NHC(H)=O^{\bullet+}$ (**FE**1) lose $C_2H_3O^{\bullet}$, CH_2O and H_2O to yield *m/z* 46 ions $HC(OH)NH_2^+$, *m/z* 59 ions $^{\bullet}CH_2N(H)CHOH^+$, and *m/z* 71 *N*-vinylformamide ions $CH_2=C(H)N(H)CHO^{\bullet+}$.

A detailed mechanistic study using the CBS-QB3 model chemistry reveals that the readily generated 1,5-H shift isomer $HOCHCH_2N(H)C(H)OH^{\bullet+}$ (**FE**2) and hydrogen-bridged radical cations (HBRCs) act as key intermediates in a 'McLafferty + 1′ type rearrangement that yields the *m/z* 46 ions. The co-generated $C_2H_3O^{\bullet}$ neutrals are predicted to be vinyloxy radicals $CH_2=CHO^{\bullet}$ in admixture with $CH_3C=O^{\bullet}$ generated by quid-pro-quo (QPQ) catalysis.

A competing C–C bond cleavage in **FE**1 leads to HBRC $[CH_2N(H)C(H)=O\cdot\cdot\cdot H\cdot\cdot\cdot O=CH_2]^{\bullet+}$, which serves as the direct precursor for CH_2O loss.

In addition, ion **FE**2 also communicates with a myriad of ion–molecule complexes of vinyl alcohol and formimidic acid whose components may recombine to form distonic ion **FE**3, $HOCH(CH_2)N(H)C(H)OH^{\bullet+}$, which loses H_2O after undergoing a 1,5-H shift. Further support for these proposals comes from experiments with D- and ^{18}O-labelled isotopologues.

Previously reported proposals for the H_2O and CO losses from protonated *N*-formylethanolamine are briefly re-examined.

1. Introduction

The well-known McLafferty rearrangement is arguably the most important hydrogen-shift rearrangement in the structure analysis of organic compounds by electron ionization (EI) mass spectrometry [1]. The reaction was discovered in the early 1950s [1c], but its detailed mechanism has been a subject of animated debate for almost 40 years. The issue of whether the γ-H transfer and α–β bond cleavage reactions occur in a *concerted* or a *step-wise* manner was not finally settled until the isotopic labelling study of Derrick and Bowie [2] left little doubt that the 1,5-H shift yields a distonic ion [3] as an intermediate.

Early investigators recognized that integrating theory and experiment would be an ideal approach to study reaction mechanisms, but this only became feasible in the late 1980s following spectacular advances in computer technology and software. The pioneering computational studies [4] of the prototypal McLafferty rearrangement in ionized *n*-butanal (using simple Hartree–Fock calculations) therefore appeared at a relatively late stage in the debate over the mechanism. Nevertheless, these studies provided crucial mechanistic information, *viz.*, the structures and energies of the key intermediates and transition-states, which cannot readily be ascertained by experiment. More recently, the Schwarz group has published a trilogy of papers [5] dealing with the dissociation of ionized valeramide. By bringing to bear sophisticated DFT (density functional theory) based calculations, the authors provided an elegant (mechanistic) rationale of a stepwise McLafferty rearrangement and three other competing dissociations, in excellent agreement with the experimental observations.

The presently available CBS [6a], Gaussian [6b] and Weizmann [6c] model chemistries often make it possible to study mechanisms with chemical accuracy (±1 kcal mol^{-1} [6d]).

In our research we have exploited these powerful tools to study dissociation mechanisms of low-energy radical cations for which experiment alone can at best provide tentative proposals [7]. This approach has led to the growing realization that rearrangements of solitary radical cations containing heteroatoms often involve hydrogen-bridged radical cations (HBRCs) [8], a subclass of ion–molecule complexes [1a], as key intermediates. HBRCs are often more stable than the incipient molecular ions and at elevated energies they may catalyze further H-transfers leading to energetically more favourable product ions or neutrals. Proton-transport

* Corresponding author. Tel.: +1 905 525 9140; fax: +1 905 522 2509.
E-mail address: terlouwj@mcmaster.ca (J.K. Terlouw).

1387-3806/$ – see front matter © 2011 Elsevier B.V. All rights reserved.
doi:10.1016/j.ijms.2011.05.011

catalysis (PTC) [9a], where, in a complex, a neutral molecule induces an ion to isomerize via a HBRC, is a prime example. An interesting variant is the catalyzed transformation of a neutral species by an ion [9b].

In the present study, we use the CBS-QB3 model chemistry [6d] to probe the dissociation of $HOCH_2CH_2NHC(H)=O^{\bullet+}$ (**FE**1), ionized *N*-formylethanolamine. This challenging ion, whose three heteroatoms make it prone to extensive hydrogen-shift rearrangements via HBRCs, has not been previously studied by either experiment or theory. It undergoes three competing fragmentations that feature in both the conventional EI and the MI (metastable ion) mass spectra: loss of $C_2H_3O^{\bullet}$, CH_2O and H_2O.

The $C_2H_3O^{\bullet}$ loss from **FE**1 points to a 'McLafferty + 1′ rearrangement in which a second H-transfer occurs following the α–β bond cleavage to produce oxygen-protonated formamide, $HC(OH)NH_2^+$. There is compelling evidence for the involvement of ion–molecule complexes in this type of rearrangement [10] and in the present system these are expected to adopt the configuration of HBRCs. This opens the possibility that PTC also plays a role in this rearrangement. Indeed, theory predicts that the neutrals of this reaction are vinyloxy radicals $CH_2{=}CHO^{\bullet}$ in admixture with acetyl radicals $CH_3C{=}O^{\bullet}$ generated by catalysis.

The competing loss of CH_2O from **FE**1 could involve a 1,6-H shift to yield the distonic ion $^{\bullet}CH_2N(H)CHOH^+$ but, here too, a very stable HBRC appears to act as a key intermediate.

Perhaps not surprisingly [7], the loss of H_2O appears to be a fairly complex multi-step reaction. It yields ionized *N*-vinylformamide, $CH_2{=}C(H)N(H)CHO^{\bullet+}$, in admixture with its more stable cyclic distonic isomer. The time-honoured approach of isotopic labelling [11] was also used to study this reaction. Analysis of various D- and ^{18}O-labelled isotopologues supports our mechanistic proposal but it also challenges theory to evaluate a bewildering array of potential exchange reactions in the key intermediates.

2. Experimental and theoretical methods

The experiments were performed with the VG Analytical ZAB-R mass spectrometer of BEE geometry (B, magnet; E, electric sector) [12a] using an electron ionization (EI) source at an accelerating voltage of 8 kV. Metastable ion (MI) and collision induced dissociation (CID) mass spectra were recorded in the second field free region (2ffr). In all collision experiments O_2 was used as the collision gas. All spectra were recorded using a PC-based data system developed by Mommers Technologies Inc. (Ottawa). Kinetic energy releases (corrected $T_{0.5}$ values) were measured according to standard procedures [13]. The *N*-formylethanolamine samples were introduced into the source (kept at 120 °C) via a standard insertion probe held at ~60 °C.

The HeI photoelectron (PE) spectrum of *N*-vinylformamide was obtained using a home-built spectrometer [12b].

The synthesis of *N*-formylethanolamine (**NFE**) from ethanolamine (Aldrich, > 99%) was performed using methyl formate (Aldrich > 99%), rather than ethyl formate as stipulated in the procedure of Tip et al. [14]. Methyl formate (100 mg, 1.7 mmol) was added slowly to a solution of ethanolamine (100 mg, 1.7 mmol) dissolved in methanol (1.8 mL) while cooling the mixture with an ice water bath. The solvent was removed under reduced pressure but the prescribed [14] vacuum distillation of the resulting high-boiling residue was not performed because it appears that 2-oxazoline (4,5-dihydro-1,3-oxazole) is generated as a persistent impurity by thermal decomposition of the sample. This point is discussed further in Section 3.2. Repeated exchanges of the labile hydrogens of N**FE** with MeOD were performed to prepare $DOCH_2CH_2NDCHO$. The D-labelled compound $HOCD_2CD_2NHCHO$ was synthesized using ethanolamine-d_4 (CDN Isotopes) in the above procedure.

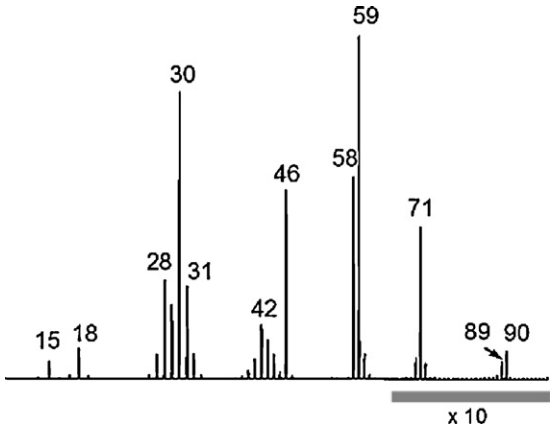

Fig. 1. EI mass spectrum of *N*-formylethanolamine $HOCH_2CH_2NHCHO$ ($M^{\bullet+} = m/z$ 89).

The D-, ^{18}O-, and mixed D/^{18}O-isotopologues $HOCH_2CH_2NHCDO$, $HOCH_2CH_2NHCH^{18}O$ and $HOCH_2CH_2NHCD^{18}O$ were prepared from the labelled methyl formates CH_3OCDO (Aldrich) $CH_3OCH^{18}O$ and $CH_3OCD^{18}O$. A 5:2:1 molar mixture of MeOH, $H_2{}^{18}O$, and (D-labelled) formic acid was kept at room temperature for ~5 days and thereafter distilled to obtain $CH_3OCH^{18}O$ and $CH_3OCD^{18}O$. *N*-formyl-*O*-methylethanolamine and its isotopologue $CH_3OCH_2CH_2NHCH^{18}O$ were synthesized from *O*-methylethanolamine (Aldrich > 99%) in a procedure analogous to that used for the preparation of **NFE**. All compounds were used without further purification.

The calculations were performed with the CBS-QB3 model chemistry [6a]. Most of the calculations were run with the Gaussian 09, Rev B.01 suite of programs [15] on the SHARCNET computer network at McMaster University. In the CBS-QB3 model chemistry the geometries of minima and connecting transition states are obtained from B3LYP density functional theory in combination with the 6-311G(2d,d,p) basis set (also denoted as the CBSB7 basis set). Computational data pertaining to the dissociation products are found in Table 1. The resulting total energies and enthalpies of formation for minima and connecting transition states (TS) in the *N*-formylethanolamine systems of ions are presented in Tables 2a and 2b. Selected optimized geometries are shown in Fig. 5. Spin contaminations ($\langle S^2 \rangle$ values of Tables 2a and 2b) were acceptable. Unless stated otherwise, all enthalpies presented in the text and in the Schemes (numbers in square brackets) refer to $\Delta_f H_{298}{}^{\circ}$ values in kcal mol^{-1} derived from the CBS-QB3 calculations. The complete set of computational results is available from the authors upon request.

3. Results and discussion

3.1. The EI mass spectrum of N-formylethanolamine and the MI and CID mass spectra of the (pseudo) molecular ions

The mass spectrum of *N*-formylethanolamine (**NFE**), see Fig. 1, displays a weak molecular ion signal (m/z 89) relative to the peaks at m/z 71, 59 and 46. These fragment ions correspond to the losses of H_2O, $CH_2{=}O$ and $C_2H_3O^{\bullet}$ and they are also observed in the MI mass spectrum of Fig. 2a. Fig. 1 also displays prominent peaks at m/z 58 and 30, which likely result from the direct bond cleavage reaction $HC(=O)NHCH_2CH_2OH^{\bullet+}$ (**FE**1) → $HC(=O)NH{=}CH_2^+$ (m/z 58) + $CH_2OH^{\bullet}$ and a subsequent partial decarbonylation of the m/z 58 ions in $CH_2NH_2^+$ (m/z 30). These ions are absent in the MI spectrum but they reappear in the CID spectrum of Fig. 2b. There-

Table 1
Energetic data derived from CBS-QB3 calculations[a] used to probe the structure and reactivity of dissociation products of ionized *N*-formylethanolamine (Fig. 4 and Scheme 3 or Scheme 4).

Species and mass		CBS-QB3 E (total) [0 K]	QB3 $\Delta_f H^\circ_{298}$	Species and mass		CBS-QB3 E (total) [0 K]	QB3 $\Delta_f H^\circ_{298}$
Fig. 4 ion **1a**	71	−246.57683	174.2	Fig. 4 ion **6a**	71	−246.51284	214.7
Fig. 4 ion **1b**$_1$	71	−246.56491	182.3	Fig. 4 ion **6b**	71	−246.51551	213.4
Sch. 3 ion **1b**$_2$	71	−246.56198	184.2	Fig. 4 ion **6c**	71	−246.51742	212.3
Fig. 4 ion **1c**	71	−246.55627	188.0	Fig. 4 ion **6d**	71	−246.54710	194.7
Fig. 4 ion **1d**	71	−246.51574	212.8	Fig. 4 ion **7a**	71	−246.52469	207.3
Fig. 4 ion **1e**	71	−246.53003	204.4	Fig. 4 ion **7b**	71	−246.54593	194.5
Fig. 4 ion **1f**	71	−246.54533	195.3	Fig. 4 ion **8a**	71	−246.46343	245.5
Fig. 4 ion **2a**	71	−246.56802	179.9	Fig. 4 ion **8b**	71	−246.50370	221.2
Fig. 4 ion **2b**	71	−246.52221	209.1	Fig. 4 ion **9**	71	−246.50699	218.0
Fig. 4 ion **3a**	71	−246.58663	167.9	TS 1a → *m/z* 70		−246.52039	209.6
Fig. 4 ion **3b**	71	−246.55412	189.0	TS 1b$_1$ → 1b$_2$		−246.55441	188.6
Fig. 4 ion **4a**	71	−246.52992	203.6	TS 1b$_1$ → 1a		−246.54987	191.0
Fig. 4 ion **4b**	71	−246.53251	202.1	TS 1b$_1$ → *m/z* 43		−246.45400	251.8
Fig. 4 ion **5a**	71	−246.53566	200.6	TS 1b$_1$ → *m/z* 43[b]		−246.50773	218.9
Fig. 4 ion **5b**	71	−246.53980	198.7	TS 1b$_2$ → 1f		−246.51782	211.4
Fig. 4 ion **5c**	71	−246.55398	189.3	TS 1f → *m/z* 43		−246.53291	203.2
Scheme 3 ion **1a**-H	70	−246.02895	153.2	HC(=NH)CH$_3$$^{\bullet+}$	43	−133.35001	230.9
$^\bullet$CH$_2$N(H)CHOH$^+$	59	−208.54478	159.2	CH$_3$C=O$^\bullet$[c]	43	−152.94205	−2.1
HC(OH)NH$_2$$^+$	46	−169.96226	124.7	CH$_2$=CHO$^\bullet$[c]	43	−152.93284	3.4
HC(=O)NH$_2$	45	−169.65356	−45.7	CH$_2$=O	30	−114.34417	−27.0
HC(=NH)OH	45	−169.63475	−34.2	CO	28	−113.18201	−26.6
CH$_2$=CHOH$^{\bullet+}$	44	−153.22216	186.2	H$_2$O	18	−76.33750	−57.0

[a] *E* (total) in Hartrees, 298 K enthalpies in kcal mol^{-1}.
[b] "Ion dipole" TS of Scheme 4.
[c] The tabulated values are in close agreement with the experimental values of −2.3 and 3.1 kcal mol^{-1} found in Refs. [19b/c].

Table 2a
Energetic data[a] from CBS-QB3 calculations of stable isomers involved in the dissociation chemistry of *N*-formylethanolamine ions **FE**1.

Species		B3LYP/CBSB7 E (total)	CBS-QB3 E (total) [0 K]	**ZPE**	QB3 $\Delta_f H^\circ_0$	QB3 $\Delta_f H^\circ_{298}$	$\langle S^2 \rangle$
NFE1a	(Scheme 5)	−323.82528	−323.24071	67.0	−83.4	−89.4	–
NFE1b	(Scheme 5)	−323.82706	−323.24156	67.3	−83.9	−90.1	–
NFE1c	(Scheme 5)	−323.82142	−323.23703	66.8	−81.1	−87.0	–
NFE1d	(Scheme 5)	−323.82683	−323.24147	67.1	−83.9	−89.9	–
NFE1e	(Scheme 5)	−323.82232	−323.23745	66.7	−81.4	−87.2	–
FE1b	(Scheme 5)	−323.50004	−322.89040	66.9	136.4	130.1	0.77
FE1d	(Scheme 5)	−323.49489	−322.89483	66.0	133.6	127.7	0.94
FE1e	(Scheme 5)	−323.48986	−322.88961	65.8	136.9	131.1	0.96
FE2a	(Scheme 7a/b)	−323.50756	−322.91103	67.1	123.5	117.2	0.76
FE2b	(Scheme 7a)	−323.50953	−322.91367	66.8	121.8	115.9	0.76
FE2c	(Scheme 7a)	−323.50920	−322.91312	66.7	122.1	116.3	0.76
FE3	(Scheme 7b)	−323.50794	−322.91411	65.9	121.5	115.7	0.76
FE4	(Scheme 7a)	−323.49180	−322.89800	66.9	131.6	125.6	0.76
FE5	(Scheme 6)	−323.47327	−322.87645	66.7	145.2	139.0	0.76
FE6	(Scheme 6)	−323.48281	−322.88688	67.1	138.6	132.7	0.78
FE7	(Scheme 9)	−323.49109	−322.89120	65.3	135.9	130.0	0.76
FE8	(Scheme 10)	−323.52560	−322.92649	67.0	113.8	107.4	0.80
FE9	(Scheme 10)	−323.51812	−322.92581	66.3	114.2	108.2	0.84
FE10	(Scheme 10)	−323.46636	−322.87536	65.2	145.8	139.8	0.77
IDC	(Scheme 7b)	−323.51318	−322.91348	65.0	121.9	116.6	0.77
LB1a	(Scheme 8)	−323.51981	−322.90252	64.3	128.8	123.6	0.77
LB1b	(Scheme 8)	−323.52181	−322.90477	64.4	127.4	122.2	0.77
HBRC1	(Scheme 7a)	−323.51259	−322.91384	64.0	121.7	116.5	0.82
HBRC2	(Scheme 7a)	−323.49539	−322.89580	64.4	133.0	127.6	0.77
HBRC3a	(Scheme 7b)	−323.52366	−322.92885	63.7	112.3	107.5	0.86
HBRC3b	(Scheme 7b)	−323.53146	−322.94155	64.8	104.3	98.9	0.84
HBRC4a	(Scheme 7a)	−323.52832	−322.92920	64.4	112.1	107.0	0.86
HBRC4b	(Scheme 8)	−323.54258	−322.93982	65.0	105.4	100.0	0.82
HBRC4c	(Scheme 8)	−323.53891	−322.93843	64.9	106.3	101.3	0.76
HBRC5a	(Scheme 6)	−323.49940	−322.90789	61.8	125.4	121.2	0.76
HBRC5b	(Scheme 6)	−323.49096	−322.90211	62.4	129.1	124.0	0.91
HBRC6	(Scheme 6)	−323.49910	−322.90335	64.1	128.3	123.6	0.78
HBRC7	(Scheme 9)	−323.51895	−322.92015	63.4	117.7	112.9	0.90
HBRC8	(Scheme 9)	−323.49969	−322.90551	63.2	126.9	121.9	0.87
HBRC9	(Scheme 9)	−323.50921	−322.91527	61.8	120.8	116.4	0.78

[a] $E_{(total)}$ in Hartrees, all other components, including the ZPE scaled by 0.99, are in kcal mol^{-1}.

Table 2b
Energetic data[a] from CBS-QB3 calculations of the connecting transition states involved in the dissociation chemistry of *N*-formylethanolamine ions **FE**1.

Species		B3LYP/CBSB7 E (total)	CBS-QB3 E (total) [0 K]	**ZPE**	QB3 $\Delta_f H_0^\circ$	QB3 $\Delta_f H_0^\circ$	$\langle S^2 \rangle$
TS **NFE**1a → b	(Scheme 5)	−323.82081	−323.23558	67.4	−80.2	−86.8	–
TS **NFE**1b → c	(Scheme 5)	−323.82041	−323.23648	66.5	−80.8	−87.0	–
TS **NFE**1c → d	(Scheme 5)	−323.82136	−323.23738	66.7	−81.3	−87.7	–
TS **NFE**1c → e	(Scheme 5)	−323.79310	−323.21054	66.5	−64.5	−71.0	–
TS **FE**1b → d	(Scheme 5)	−323.47975	−322.88220	65.5	141.6	135.2	0.76
TS **FE**1b → e	(Scheme 5)	−323.47121	−322.87311	64.8	147.3	141.3	0.78
TS **FE**1b → 2a	(Scheme 7a)	−323.48963	−322.89026	65.8	136.5	130.3	0.78
TS **FE**1b → 6	(Scheme 6)	−323.40192	−322.81344	63.0	184.7	178.7	0.79
TS **FE**1b → 7	(Scheme 10)	−323.46028	−322.86744	62.5	150.8	144.6	0.80
TS **FE**1b → 9	(Scheme 10)	−323.45826	−322.86223	63.0	154.1	147.5	0.76
TS **FE**1b → HBRC1	(Scheme 7a)	−323.48772	−322.88549	64.3	139.5	133.4	0.77
TS **FE**1e → 5	(Scheme 6)	−323.46057	−322.86376	66.4	153.1	147.0	0.76
TS **FE**2a → b	(Scheme 7a)	−323.48601	−322.89432	65.7	133.9	127.9	0.76
TS **FE**2a → 3	(Scheme 7b)	−323.48746	−322.88894	64.8	137.3	131.5	0.77
TS **FE**2a → 10	(Scheme 10)	−323.46304	−322.87033	63.0	149.0	142.7	0.76
TS **FE**2b → c	(Scheme 7a)	−323.50061	−322.90787	65.9	125.4	119.4	0.76
TS **FE**2b → HBRC2	(Scheme 7a)	−323.49387	−322.89520	64.2	133.4	127.6	0.77
TS **FE**2c → 4	(Scheme 7a)	−323.47197	−322.88049	64.1	142.6	136.3	0.76
TS **FE**3 → 7	(Scheme 9)	−323.48386	−322.89105	63.2	136.0	129.4	0.79
TS **FE**3 → 10	(Scheme 10)	−323.46103	−322.87167	65.4	148.2	141.6	0.79
TS **FE**3 → IDC	(Scheme 7b)	−323.48684	−322.89275	64.4	134.9	128.6	0.76
TS **FE**4 → HBRC4	(Scheme 7a)	−323.47133	−322.87227	64.5	147.8	141.8	0.93
TS **FE**5 → 6	(Scheme 6)	−323.47395	−322.88016	65.1	142.8	136.4	0.77
TS **FE**5 → HBRC5a	(Scheme 6)	−323.45533	−322.84521	63.3	164.8	159.3	0.76
TS **FE**6 → HBRC6	(Scheme 6)	−323.48119	−322.88215	65.5	141.6	135.7	0.76
TS **FE**7 → HBRC9	(Scheme 9)	−323.47504	−322.88060	63.9	142.6	136.2	0.78
TS **FE**8 → 9	(Scheme 10)	−323.46838	−322.87663	65.9	145.0	138.6	0.76
TS **IDC** → HBRC3a	(Scheme 7b)	−323.50905	−322.91927	63.6	118.3	113.1	0.82
TS **IDC** → FE8	(Scheme 10)	−323.51190	−322.91028	66.0	123.9	117.6	0.77
TS **LB**1a → 1b	(Scheme 8)	−323.50549	−322.89145	63.4	135.7	130.3	0.78
TS **LB**1b → HBRC4c	(Scheme 8)	−323.51333	−322.89953	63.0	130.7	125.3	0.78
TS **HBRC**2 → 4	(Scheme 7a)	−323.49204	−322.89453	64.1	133.8	128.3	0.77
TS **HBRC**3a → b	(Scheme 7b)	−323.50544	−322.91285	63.8	122.3	116.8	0.78
TS **HBRC**3a → 7	(Scheme 9)	−323.50662	−322.90980	63.1	124.2	118.2	0.91
TS **HBRC**3a → 8	(Scheme 9)	−323.47406	−322.87975	64.0	143.1	137.7	0.82
TS **HBRC**4a → b	(Scheme 8)	−323.51051	−322.91368	63.3	121.8	116.5	0.85
TS **HBRC**4b → LB1a	(Scheme 8)	−323.49055	−322.89100	60.2	136.0	130.3	0.79
TS **HBRC**4b → c	(Scheme 8)	−323.47228	−322.87312	62.3	147.3	141.9	0.77
TS **HBRC**5a → b	(Scheme 6)	−323.48681	−322.89611	62.6	132.8	127.7	0.83

[a] $E_{(total)}$ in Hartrees, all other components, including the ZPE scaled by 0.99, are in kcal mol^{-1}.

fore, an important precondition imposed by experiment on theory is that enthalpies of stable intermediates, connecting transition states and dissociation thresholds of proposed dissociation mechanisms of the *metastable* ions should not exceed 157 kcal mol^{-1}, the calculated $\Sigma\Delta_f H$ value of the direct bond cleavage products HC(=O)NH=CH$_2^+$ + CH$_2$OH$^\bullet$.

The conspicuous peak at *m*/*z* 90 in Fig. 1 represents [M + H]$^+$ ions resulting from the remarkably efficient self-protonation of **NFE** by chemical ionization: raising the source pressure from *c*. 3×10^{-7} to 1×10^{-6} Torr, by gently heating the sample, causes the *m*/*z* 90: 89 peak intensity ratio to increase to ~10:1! In line with this, our calculations show that the various proton transfer reactions between **FE**1 and its neutral **NFE** are exothermic: the proton affinity (PA) of **NFE** is 214 kcal mol^{-1} but those of O=C$^\bullet$–NHCH$_2$CH$_2$OH, HC(=O)NH–C$^\bullet$HCH$_2$OH, HC(=O)NH–CH$_2$C$^\bullet$HOH, HC(=O)NHCH$_2$CH$_2$O$^\bullet$ and HC(=O)N$^\bullet$CH$_2$CH$_2$OH are only 190, 187, 187, 203 and 204 kcal mol^{-1}, respectively.

The MI and CID mass spectra of protonated *N*-formylethanolamine (**PFE**), see Fig. 2c and d, are dominated by peaks at *m*/*z* 62 and 72, corresponding to the losses of CO and H$_2$O. The associated reaction mechanisms have been briefly addressed by Tip et al. [14] in their study of *N*-formylethanolamine as a matrix for the Fast Atom Bombardment analysis of non-polar compounds, including saccharides. One point that was not addressed concerns the notable peaks at *m*/*z* 71, 59 and 46 in the CID spectrum of Fig. 2d. That these peaks do not originate from the naturally occurring ^{13}C-isotopologue of **FE**1 follows from the fact that the CID spectrum of Fig. 2d does not change with the *m*/*z* 90:89 peak ratio. Their presence suggests that **PFE** may lose H$^\bullet$ to produce an *m*/*z* 89 ion having dissociation characteristics akin to those of **FE**1.

The next Section (3.2) deals with the structures of the *m*/*z* 71, 59 and 46 product ions generated from (metastable) ions **FE**1. Sections 3.3–3.5 present a conformational and mechanistic analysis of the dissociation chemistry of ions **FE**1 and D- and ^{18}O-labelled isotopologues. Section 3.6 re-examines the previously reported dissociation mechanisms [14] of *protonated N*-formylethanolamine.

3.2. Identification of the product ions generated in the dissociation of ions *FE*1

A comparison of the CID mass spectra of the *m*/*z* 59 and 46 product ions, see Fig. 3a and b with reference spectra [16,17] leaves little doubt that the distonic ion HC(OH)NH=CH$_2^{\bullet+}$ (*m*/*z* 59) and oxygen-protonated formamide HC(OH)NH$_2^+$ (*m*/*z* 46) are generated.

Using the values from Table 1, we find that the sum of the enthalpies of HC(OH)NH=CH$_2^{\bullet+}$ and CH$_2$=O ($\Sigma\Delta_f H$ = 132 kcal mol^{-1}) is well below the upper limit of 157 kcal mol^{-1} imposed by experiment. Using this energy criterion, we can safely conclude that formaldehyde is lost rather

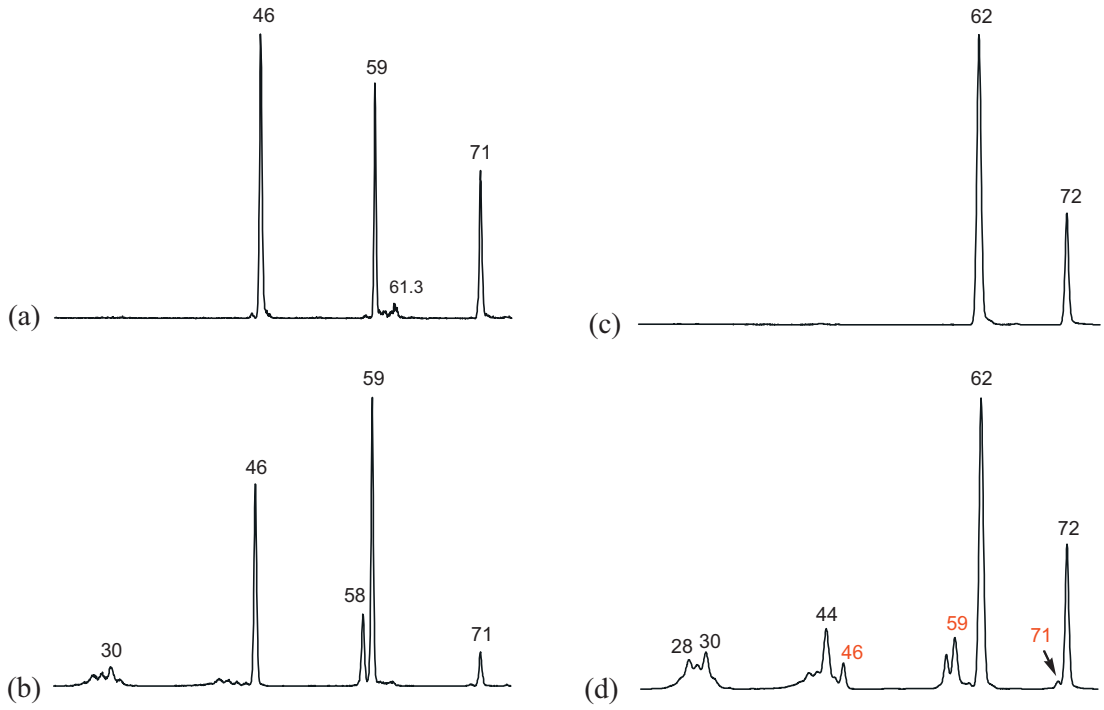

Fig. 2. (a) MI and (b) CID mass spectra of the *N*-formylethanolamine radical cation (**FE**1); (c) MI and (d) CID mass spectra of protonated *N*-formylethanolamine (**PFE**); note: a weak peak (*c.* 5%) at *m*/*z* 89 in Fig. 2d is not shown.

than its elusive hydroxycarbene isomer HCOH [18], which lies considerably higher in energy.

In contrast, the structure of the mass 43 neutral is not so easily ascertained because the enthalpies of $CH_3C{=}O^{\bullet}$ and $CH_2{=}CHO^{\bullet}$ are close, see Table 1. Moreover, the combined enthalpies $\Sigma\Delta_f H$ $[HC(OH)NH_2^+ + CH_3C{=}O^{\bullet}] = 124$ kcal mol^{-1} and $\Sigma\Delta_f H$ $[HC(OH)NH_2^+ + CH_2{=}CH{-}O^{\bullet}] = 129$ kcal mol^{-1} both satisfy the energy criterion discussed in Section 3.1.

A recent computational study [19a] predicts that the other isomers $CH_2{=}C{-}OH^{\bullet}$ and $CH{=}CH{-}OH^{\bullet}$ lie 29 and 33 kcal mol^{-1} higher than the acetyl radical global minimum and thus can be excluded from our analysis. Unfortunately, a CIDI experiment [20] to probe the structure of the $C_2H_3O^{\bullet}$ radical could not be realized due to insufficient signal intensity. The intriguing possibility that both $CH_3CO^{\bullet}$ and $CH_2{=}CHO^{\bullet}$ isomers are co-generated is discussed in Section 3.4.

Establishing the structure of the *m*/*z* 71 product ion is not straightforward because there is a dearth of information on the $C_3H_5NO^{\bullet+}$ system of ions [13] and very few CID mass spectra have been reported [21a]. Fig. 4 shows potential *m*/*z* 71 product ion structures and their associated CBS-QB3 derived 298 K enthalpies. These will be used as a guide in the analysis of the CID mass spectrum of Fig. 3c.

As pointed out in Section 3.1, the combined enthalpy of $C_3H_5NO^{\bullet+} + H_2O$ must not exceed 157 kcal mol^{-1}. Using $\Delta_f H$ $(H_2O) = -58$ kcal mol^{-1}, an upper limit of 215 kcal mol^{-1} is obtained for $\Delta_f H$ $(C_3H_5NO^{\bullet+})$, so that ions **8a**, **8b** and **9** can be ruled out as viable candidates.

The most attractive of the remaining structures is the very stable *N*-vinylformamide ion **1b**. Its CID spectrum appears to be close to that of Fig. 3c, but it does not display the prominent, narrow *m*/*z* 41 peak and its *m*/*z* 43 peak is considerably more intense.

We are confident, however, on the basis of the arguments presented below, that a mixture of ions **1b** and its cyclic distonic isomer **1a** (see Fig. 4), is generated in the H_2O loss.

First, the discrepancy in the relative intensity of the *m*/*z* 43 peaks appears to be due to the fact that they represent both collision-induced and spontaneous dissociations. When the unimolecular component (whose intensity strongly depends on the internal energy of the precursor ions) is removed by applying an external voltage (−1 kV) to the collision cell [22], the spectra of Fig. 3e and f are obtained. It is gratifying to observe that the *m*/*z* 42: 43 peak ratios are now virtually the same. In fact, the more intense *m*/*z* 41 peak of Fig. 3f, which may consist of a narrow and a broad component, and the more prominent charge-stripping peak (++) are the only distinguishing features.

Second, we propose that the narrow part of the *m*/*z* 41 peak of Fig. 3f results from thermal decomposition because its intensity appeared to vary during the evaporation of the sample. Indeed, the CID spectrum of the *m*/*z* 71 ions obtained from a sample that had been subjected to prolonged heating (at 100 °C for 8 h), see Fig. 3d, is dominated by a narrow *m*/*z* 41 peak. A plausible thermal decomposition product, see Scheme 1, is 2-oxazoline (**4a**), whose CID spectrum [21b] is very close to that of Fig. 3d.

In this context, we note that experiments with $HOCH_2CH_2NHCH^{18}O$ indicate that the thermal decomposition involves a specific loss of $H_2{}^{18}O$: the CID spectrum of the resulting *m*/*z* 71 ions (not shown) displays an intense, narrow peak at *m*/*z* 41 whereas the CID spectrum of the *m*/*z* 73 ions shown in Fig. 3h, does not.

This leads us to conclude that the *m*/*z* 73 ions are generated by the specific loss of $H_2{}^{16}O$ from the ^{18}O-labelled radical cations **FE**1. Indeed, a comparison of Fig. 3e and h provides strong evidence that ions **1b** are generated because the *m*/*z* 41–43 peak clusters

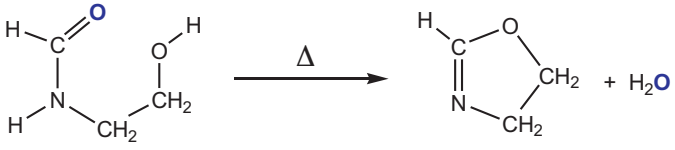

NFE1 **2-oxazoline**

Scheme 1.

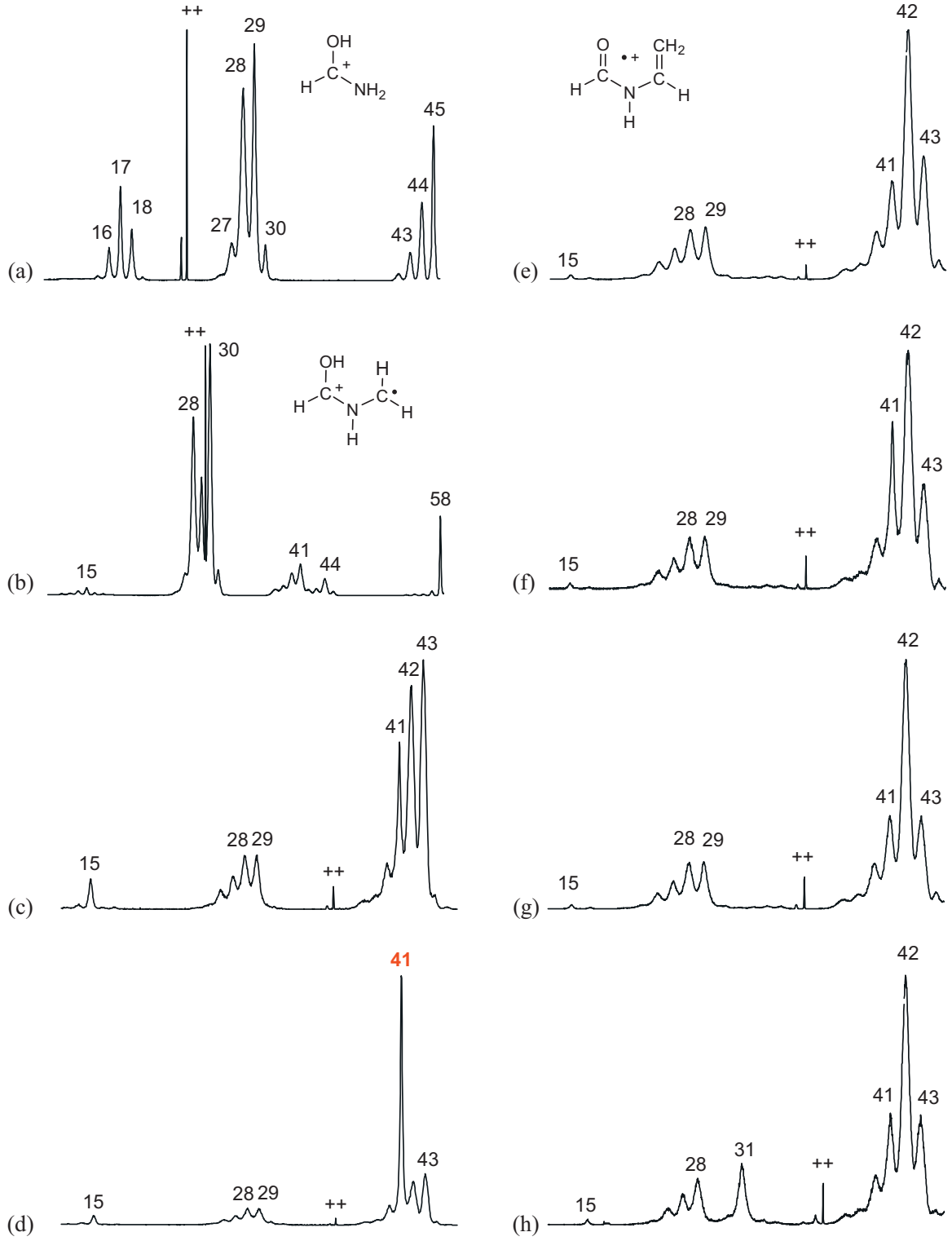

Fig. 3. Left column: (a), (b) and (c) are CID mass spectra of the source generated *m*/*z* 46, *m*/*z* 59 and *m*/*z* 71 ions from *N*-formylethanolamine; (d) CID spectrum of the *m*/*z* 71 ions generated by thermal decomposition.
Right column: CID spectra with the collision chamber at −1 kV of *m*/*z* 71 ions generated from (e) *N*-vinyl-formamide; (f) *N*-formylethanolamine and (g) *N*-formyl-O-methylethanolamine $CH_3OCH_2CH_2NHCHO$; (h) CID spectrum of the *m*/*z* 73 ions generated from ^{18}O-labelled *N*-formylethanolamine $HOCH_2CH_2NHCH^{18}O$.

are almost identical and the shift of *m*/*z* 29–31 confirms the HCO structure motif.

Complementary evidence that ions **1b** are generated comes from an analysis of *N*-formyl-O-methylethanolamine (**NOE**). As shown in Scheme 2, ion **NOE** readily loses the methoxy oxygen atom (in the form of CH_3OH) to generate ions of *m*/*z* 71.

The CID spectrum of the *m*/*z* 71 ions, see Fig. 3g, is virtually the same as those of Fig. 3e and f, indicating that ions **FE**1 and **NOE** dissociate into **1b** via analogous mechanisms. Note that the analogous thermal decomposition of Scheme 1 does not occur in **NOE** as witnessed by the spectrum of Fig. 3g, which shows no trace of a narrow component in the *m*/*z* 41 peak.

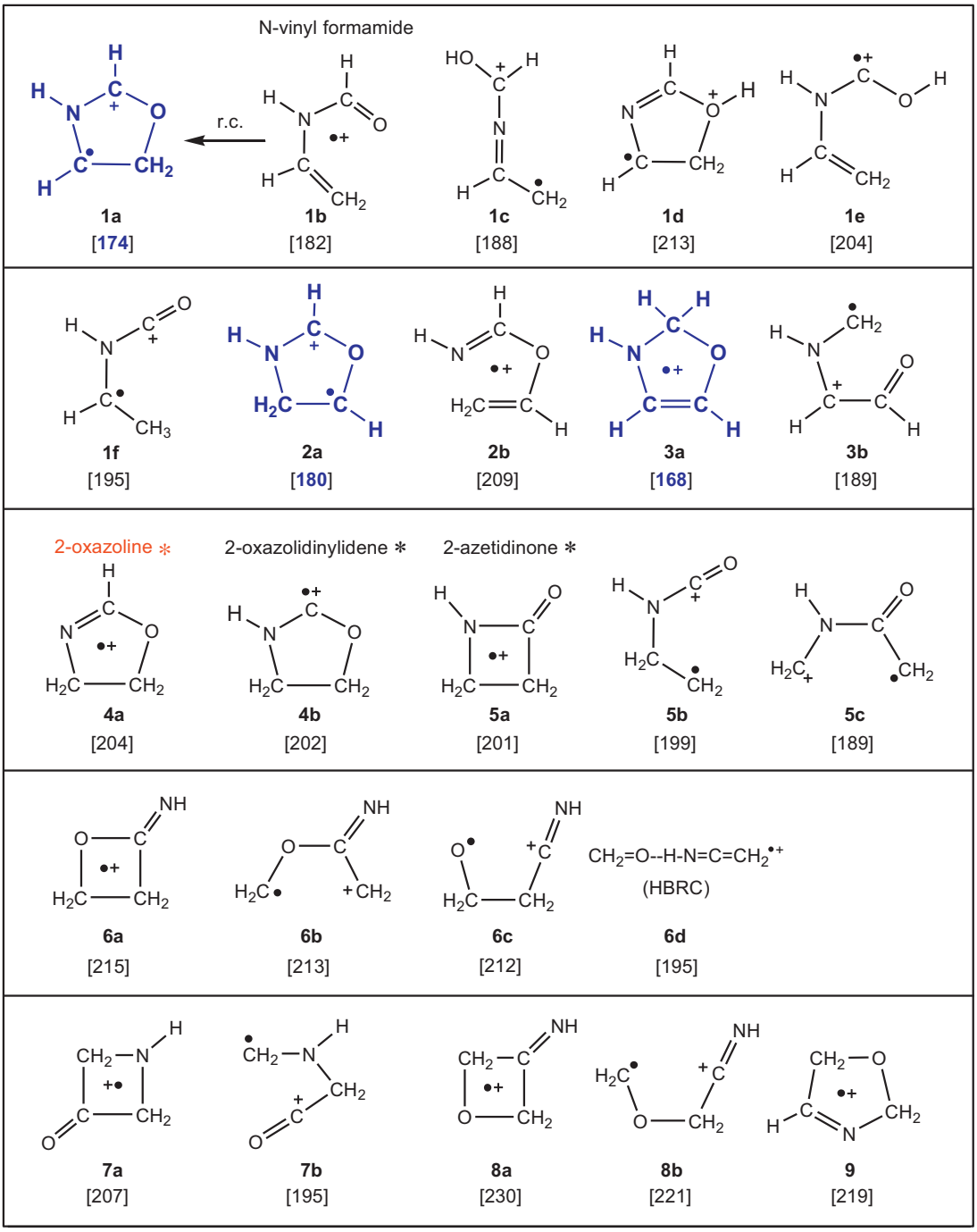

Fig. 4. $C_3H_5NO^+$ (m/z 71) ion structures and their 298 K enthalpies of formation in kcal mol^{-1} derived from CBS-QB3 calculations; * For these ions, the CID mass spectra have been reported [21a].

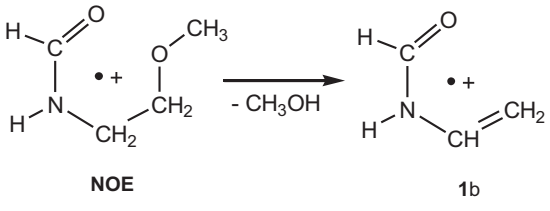

Scheme 2.

A subtle difference between the CID spectra of ion **1b** (Fig. 3e) and the **FE**1 derived ions (Fig. 3f) is the enhanced charge-stripping peak at m/z 35.5 in Fig. 3f.

This prompted us to consider the co-generation of the cyclic counterpart of ion **1b**, the remarkably stable distonic ion **1a** of Fig. 4. Distonic ions are often more prone to charge-stripping, especially with O_2 as collision gas, and in line with this, our calculated vertical IE of **1a** (13.6 eV) is considerably lower than that of **1b** (16.3 eV).

Nevertheless, the proposal that the spectrum of Fig. 3f is compatible with a mixture of ions **1a** and **1b** hinges on the question whether the two isomers have closely similar CID characteristics. The CID spectrum of pure ions **1a** is not accessible, but the following computational analysis indicates that this is indeed the case.

Scheme 3 summarizes our computational results on metastable ions **1b**, which generate both *m*/*z* 43 and *m*/*z* 70 ions. We propose that the H• loss does not occur from ion **1b** directly, but rather from its cyclic distonic isomer **1a**: the transformation **1b** → **1a** involves a facile ring-closure via a TS (at 191 kcal mol^{-1}) that lies well below the dissociation threshold at 205 kcal mol^{-1}. In contrast, direct H• loss reactions from ion **1b** to form CH_2=CH−NH−$^{+}$C=O, $^{+}CH_2$−CH=N−CH=O or CH_2=C^{+}−NH−CH=O have $\Sigma\Delta_f H$ values of 236, 234 and 245 kcal mol^{-1} and are thus far more energy demanding!

The competing formation of the *m*/*z* 43 ion involves loss of CO: the identity of the neutral was established by a CID experiment on the isotopologue HC(=O^{18})NHCH=CH_2. A previous theoretical study [23] indicates that ionized formamide

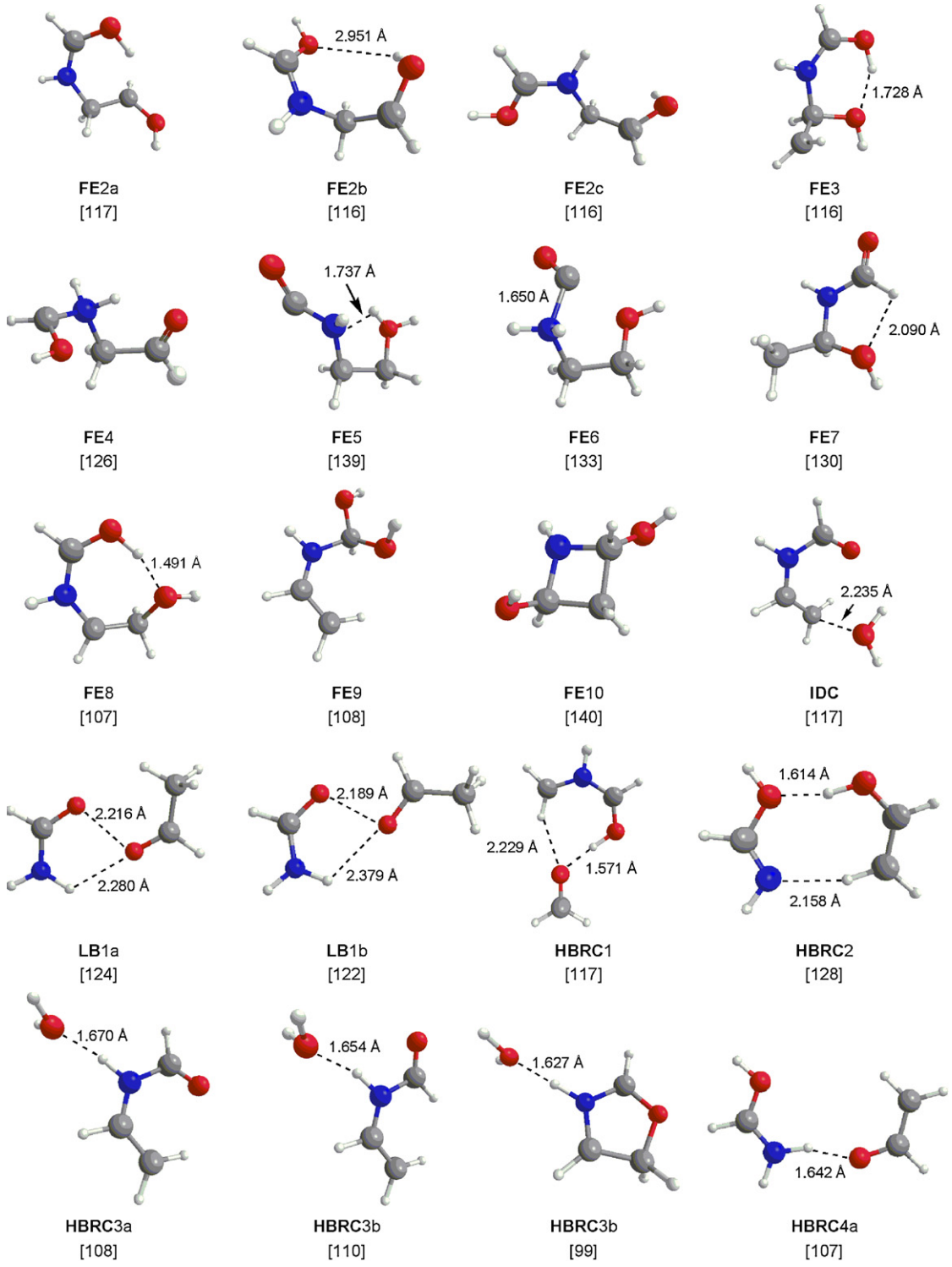

Fig. 5. Optimized geometries of selected minima and transition states involved in the dissociation chemistry of ionized *N*-formylethanolamine. Numbers in brackets are CBS-QB3 derived 298 K enthalpies in kcal mol^{-1}.

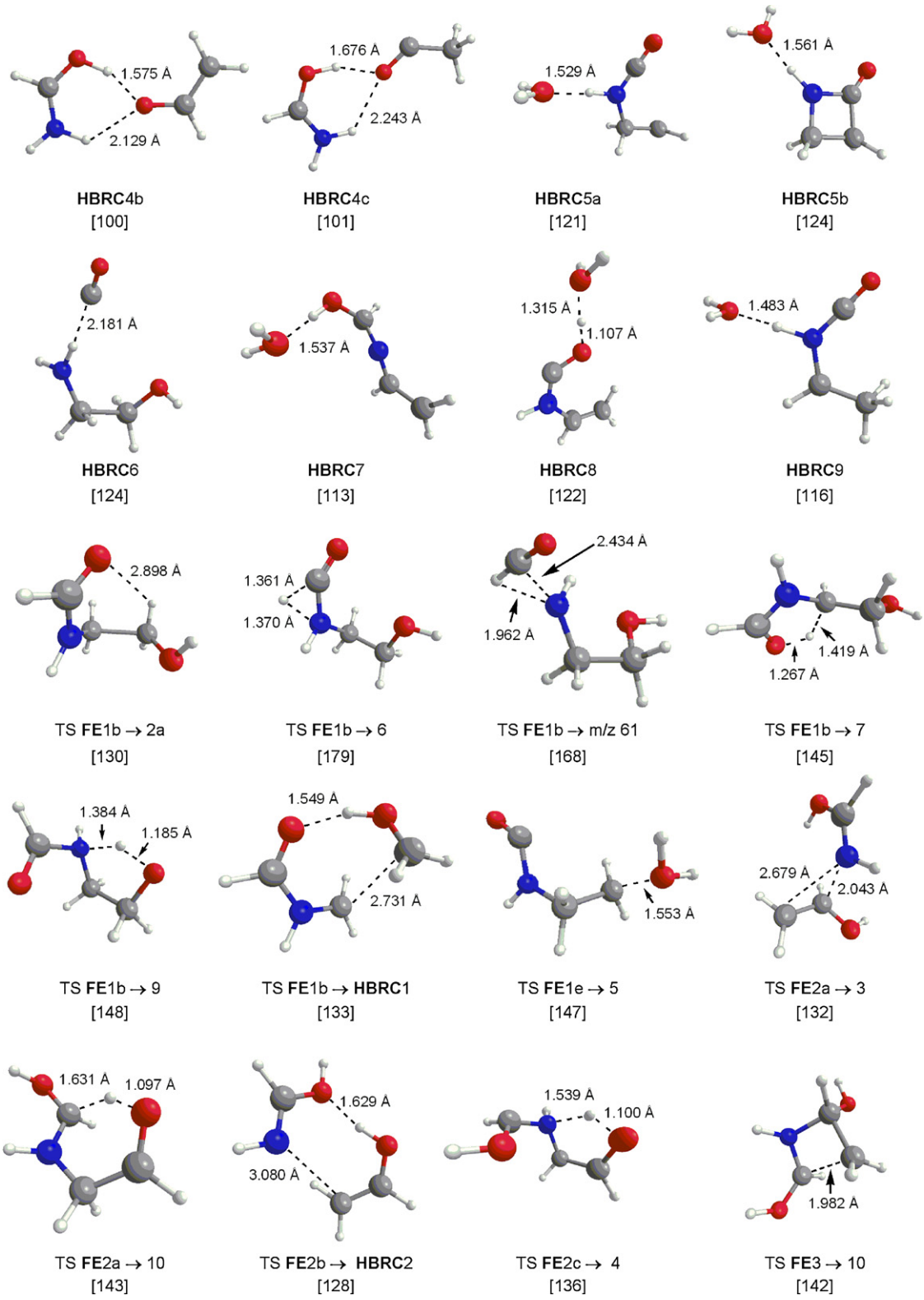

Fig. 5. (*Continued*)

undergoes decarbonylation via an ion–dipole complex accessible from the first excited state, rather than a classical 1,2-H shift. Although the energy difference between the first two bands of the PE spectrum of *N*-vinylformamide is larger than that of formamide (1.0 vs. 0.2 eV), it seemed worth considering whether ions **1b** also decarbonylate via an excited state. Scheme 4 shows the optimized geometries of the classical 1,2-H shift and ion–dipole type transition states. Both are quite energy demanding with enthalpies of 252 and 220 kcal mol^{-1} respectively.

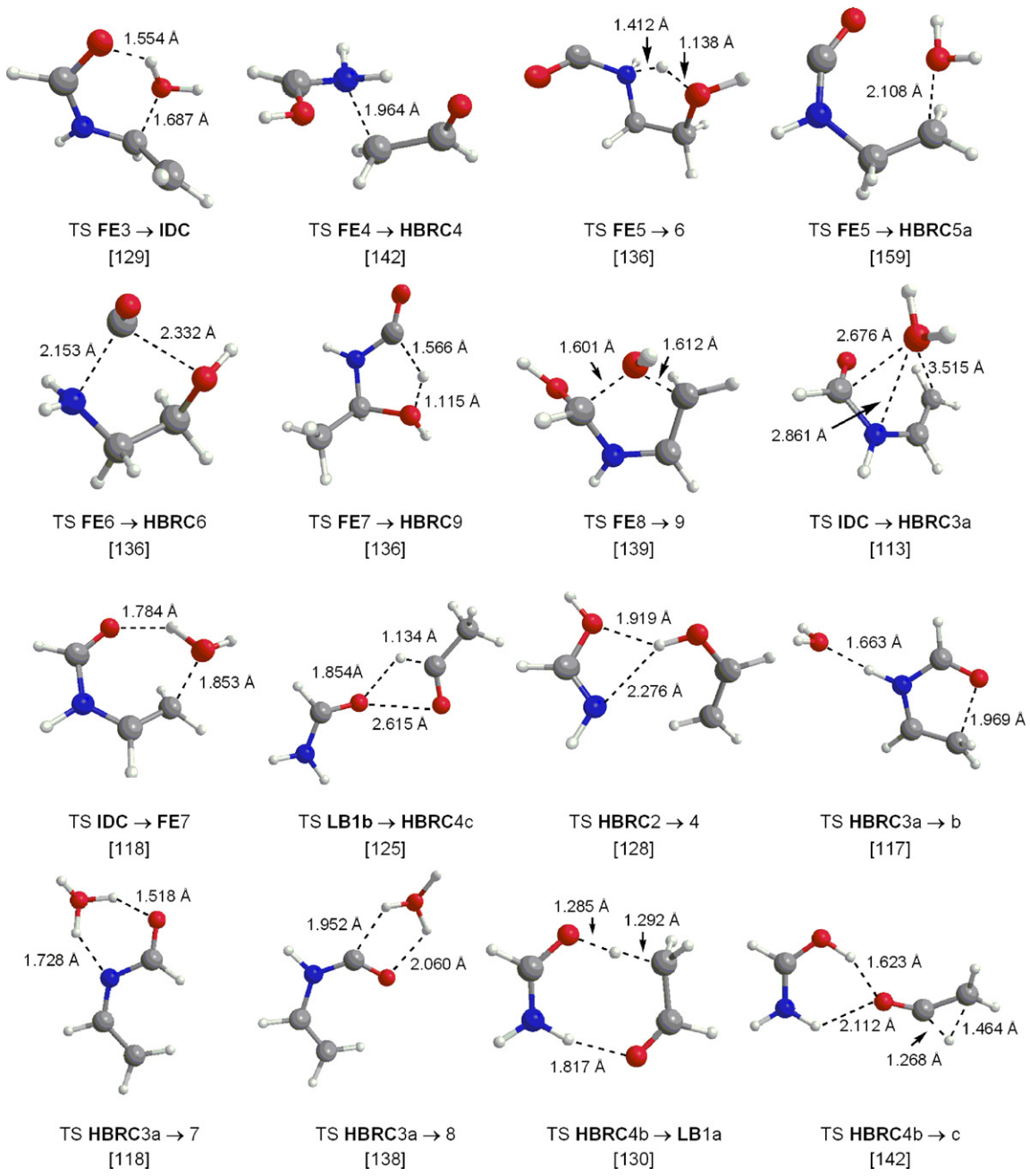

Fig. 5. (*Continued*)

A more attractive decarbonylation route involves the 1,4-H shift connecting ions $\mathbf{1b}_2$ and **1f** of Scheme 3. Loss of CO from **1f** yields the *m*/*z* 43 acetimine ion $CH_3C(=NH)H^{\bullet+}$.

An important result from the above computational analysis is that the TS connecting ions **1a** and **1b** lies ~15–20 kcal mol^{-1} below the dissociation thresholds for the losses of H$^{\bullet}$ and CO. This implies that a significant fraction of the stable ions **1a**/**b** may interconvert and that, apart from the charge-stripping peak, their CID mass spectra may not be significantly different. Thus, the CID spectrum of Fig. 3f may well represent a mixture of **1a** and **1b**.

3.3. Conformational analysis of neutral and ionized *N*-formylethanolamine

Before addressing the proposed mechanisms, we will first consider the various conformers of neutral and ionized *N*-formylethanolamine. This is relevant in view of the *E*/*Z*-type isomerism of the amide functionality [24], whose barrier may greatly exceed that of a McLafferty-type 1,5-H shift.

The calculations of Scheme 5 (bottom) indicate that the O–H–O and N–H–O bridged **NFE** conformers **1b** and **1d** are a few kcal mol^{-1} more stable than the non-bridging neutrals **1a**, **1c** and **1e**. The barriers connecting **1a**, **1b**, **1c** and **1d** are marginal, but rotation of the C–N amide bond **NFE**1c → 1e, and the associated disturbance of the π-system [24], requires 16 kcal mol^{-1}! This would imply that **1b** and **1d** are the principal species among the freely equilibrating *Z*-conformers and that the less stable *E*-conformer **NFE**1e may also be present in the sample.

The corresponding ionic conformers are shown in the top part of Scheme 5. Ion **FE**1a is not a minimum but instead it rearranges to the distonic ion **FE**2 via a 1,5-H shift. This reaction will be discussed in the next section. Ion **FE**1c is not a minimum either: it rotamerizes to **FE**1b.

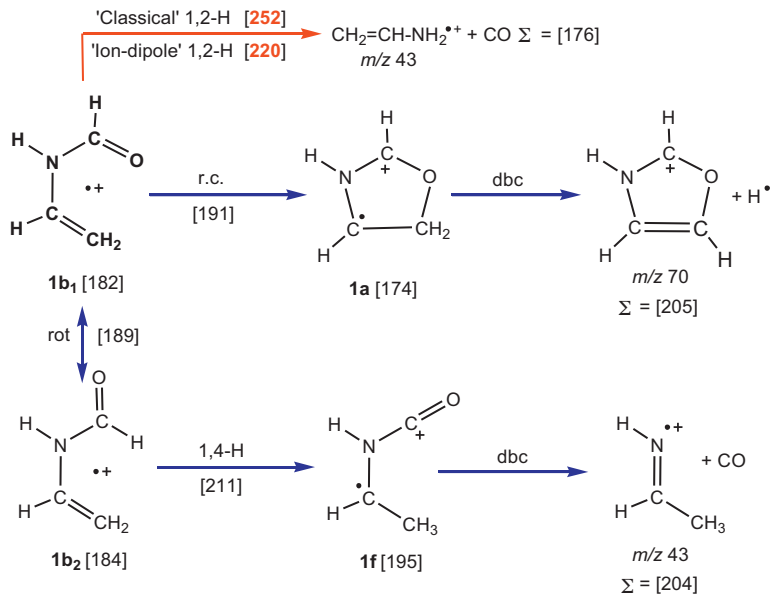

Scheme 3. Mechanistic proposals for the loss of CO and H• from *N*-vinylformamide ions **1b**. The numbers are CBS-QB3 derived 298 K enthalpies in kcal mol^{-1}.

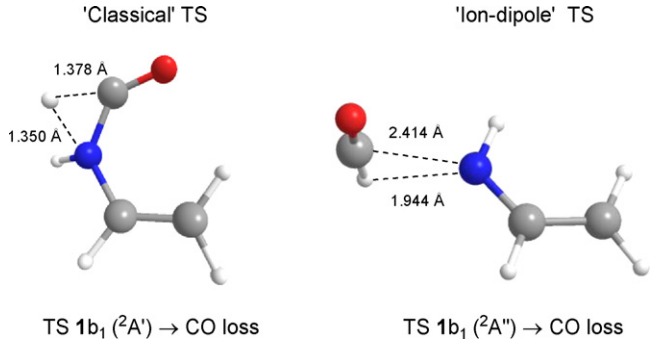

Scheme 4. Optimized geometries of the transition states for the loss of CO from the A′ and A″ states of the *N*-vinylformamide ion **1b**.

Prima facie, it is surprising that the O–H–O bridge is broken upon ionization of **NFE**1b. However, a charge-distribution analysis indicates that the amide moiety is ionized, which would repel the bridging proton.

Ions **FE**1b and **FE**1d are separated by a negligible barrier but, as with the neutrals, the rotation of the amide bond **FE**1b → 1e is energy demanding. This raises the possibility that the dissociation chemistry of **FE**1e differs from that of conformers **FE**1b/d.

Scheme 6 explores the *a priori* plausible H_2O loss from conformer **FE**1e. A 1,5-H shift in **FE**1e would produce distonic ion **FE**5, which may further rearrange into **HBRC**5a by cleaving the C–OH_2^+ bond. The subsequent loss of H_2O from **HBRC**5a, or its ring-closed isomer **HBRC**5b, would produce ions **5a** and **5b** respectively. However, the C–OH_2^+ bond cleavage is surprising high, which makes this an unrealistic proposal.

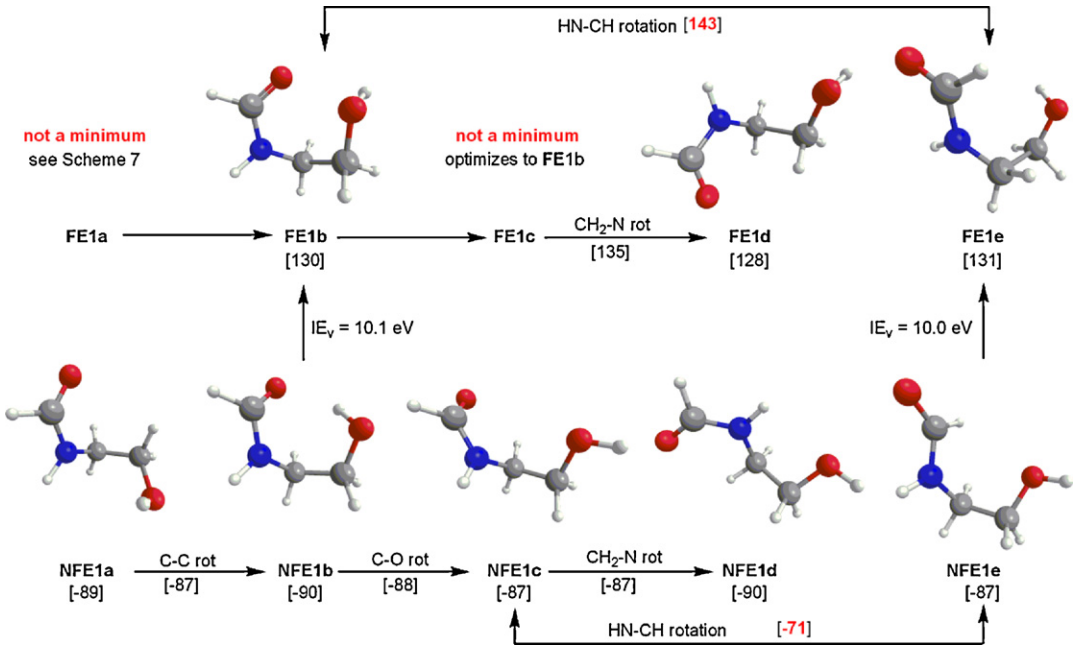

Scheme 5. Conformers of neutral (**NFE**) and ionized (**FE**) *N*-formylethanolamine. Numbers in brackets are CBS-QB3 derived 298 K enthalpies of formation in kcal mol^{-1}. IE_v is the calculated vertical ionization energy.

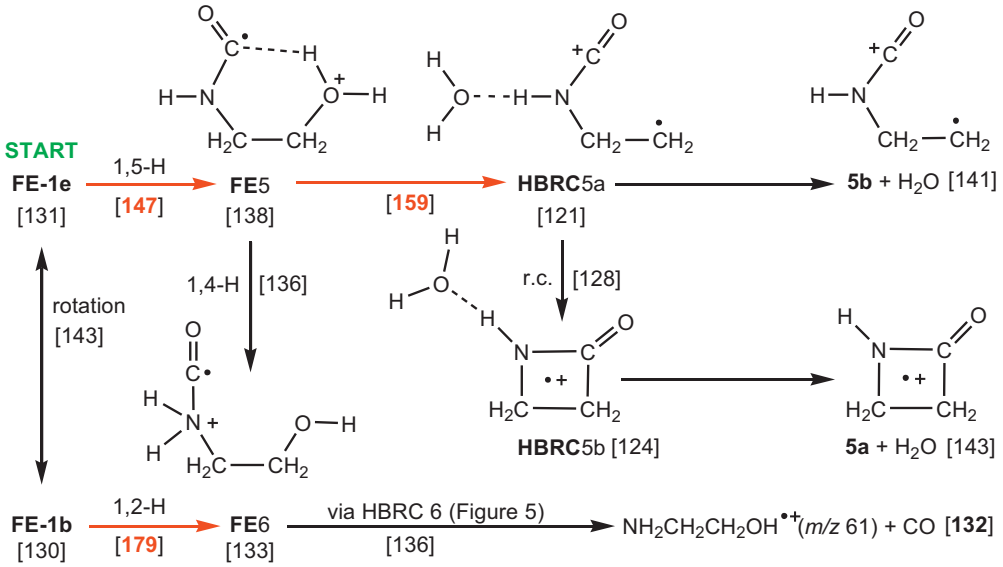

Scheme 6. Plausible mechanisms for the H_2O loss from the ionized *N*-formylethanolamine conformer **FE**1e, in conjunction with the non-observed decarbonylation. The numbers refer to 298 K enthalpies (in kcal mol^{-1}) derived from CBS-QB3 calculations.

Experiment supports this conclusion because the CID spectrum of ion **5a**, the 2-azetidinone ion, is dominated by *m/z* 28 [21a] and the same is undoubtedly true for **5b**.

Scheme 6 also predicts that the decarbonylation route **FE**5 → **FE**6 → $NH_2CH_2CH_2OH^{\bullet+}$ (*m/z* 61) + CO lies well below the critical energy for the 1,5-H shift **FE**1e → **FE**5. However, the MI spectrum of Fig. 2a shows that decarbonylation does **not** occur. The spectrum does contain a minor peak at *m/z* 61 but its non-integral position on the energy scale (*m/z* 61.3) betrays its identity as an interference peak [25] originating from the protonated precursor molecule.

That the decarbonylation does not occur is because the prerequisite 1,5-H shift requires some 4 kcal mol^{-1} more energy than the rotation of **FE**1e to **FE**1b/d. In the next Section it is shown that conformer **FE**1b initiates the losses of H_2O, CH_2O and $C_2H_3O^{\bullet}$.

3.4. The proposed mechanisms for the losses of CH_2O, $C_2H_3O^{\bullet}$ and H_2O from ionized N-formylethanolamine

The energy diagrams of Scheme 7 summarize our proposed mechanisms starting from conformer **FE**1b.

The calculations predict that vertical ionization of **NFE**1b yields vibrationally excited ions **FE**1b at an energy level (144 kcal mol^{-1}) that lies well above the low TS (133 kcal mol^{-1}) for the dissociation route **FE**1b → **HBRC**1 → $CH_2N(H)CHOH^{\bullet+}$ (*m/z* 59) + CH_2O, of Scheme 7a. This scenario is consistent with the fact that the molecular ion in the EI mass spectrum of Fig. 1 is very weak relative to the *m/z* 59 base peak. Likewise, the deep potential well occupied by **HBRC**1 would explain the high relative intensity of the *m/z* 59 peak in the MI spectrum, c. 10% of the precursor ion beam. Since the *m/z* 46 and 71 peaks of this spectrum have comparable intensities, the key transition states of their proposed generation should not significantly exceed the TS for the CH_2O loss at 133 kcal mol^{-1}. It will be seen that this is indeed the case.

The loss of a $C_2H_3O^{\bullet}$ radical from ion **FE**1 formally results from the consecutive transfer of two hydrogens in a process coined the "McLafferty + 1″ rearrangement [1]. In the first step of the mechanism, **FE**1b rotamerizes to **FE**1a, which spontaneously undergoes a γ-H shift to produce the distonic ion **FE**2a. A reasonable proposal for the second H-transfer involves the classical 1,4-H shift **FE**2c → **FE**4, shown in the inset of Scheme 7a. However, its minimum energy requirement (12 kcal mol^{-1}) is so much higher than that of the CH_2O loss (3 kcal mol^{-1}) that competition becomes unlikely.

Inspired by the proposal that ion–molecule complexes can play an important role in the McLafferty + 1 mechanism [10], we have explored the possibility that HBRCs are generated from **FE**2a. Indeed, the calculations of Scheme 7a show that conformer **FE**2b may cleave at the C–N bond to yield the remarkably stable ion **HBRC**2. Transfer of a proton from the vinyl alcohol moiety of **HBRC**2 to the amide nitrogen leads to the even more stable N–H–O bridged species **HBRC**4a, which may dissociate into $HC(OH)NH_2^+$ (*m/z* 46) + CH_2=CHO$^{\bullet}$.

We note that the computed transition-state energies involved in this HBRC mediated reaction lie below the enthalpy of **FE**1 so that the reaction is without a net barrier!

The above proposal implies that the vinyloxy radical CH_2=CHO$^{\bullet}$ is lost in the dissociation, but an intriguing question is whether the more stable isomer $CH_3CO^{\bullet}$ is also generated, as is the case with the 1-methoxy-2-propanol ion [26]. As mentioned above, it was not possible to probe this by experiment and so we have turned to the calculations of Scheme 8, which uses **HBRC**4a of Scheme 7 as the starting point, to shed light on this question.

Scheme 8 indicates that the 1,2-H shift in the CH_2=CHO$^{\bullet}$ component of **HBRC**4b that leads to **HBRC**4c is not feasible because its TS lies 13 kcal mol^{-1} above the dissociation threshold $HC(OH)NH_2^+$ + CH_2=CHO$^{\bullet}$. However, the 1,2-H shift barrier may be lowered significantly if protonated formamide acts as a catalyst. In this scenario, the protonated formamide component of **HBRC**4b transfers a hydrogen to the methylene carbon of CH_2=CHO$^{\bullet}$, to produce ion **LB**1a, a two center, 3-electron bonded complex [27] comprising formamide and acetaldehyde. The subsequent transformation **LB**1a → **LB**1b may be viewed as a simple rotation of the $CH_3C(H)$=O component. This orients the aldehydic hydrogen so that it may be transferred back to the formamide moiety to generate **HBRC**4c, which decomposes into CH_3C=O$^{\bullet}$ and $HC(OH)NH_2^+$, the 'regenerated' catalyst.

This route reduces the barrier for the transformation CH_2=CHO$^{\bullet}$ → CH_3C=O$^{\bullet}$ from 42 to 30 kcal mol^{-1} so that it now lies within 1 kcal mol^{-1} of the dissociation threshold $HC(OH)NH_2^+$ + CH_2=CHO$^{\bullet}$. As a result, a fraction of the $C_2H_3O^{\bullet}$ radicals lost may be CH_3C=O$^{\bullet}$.

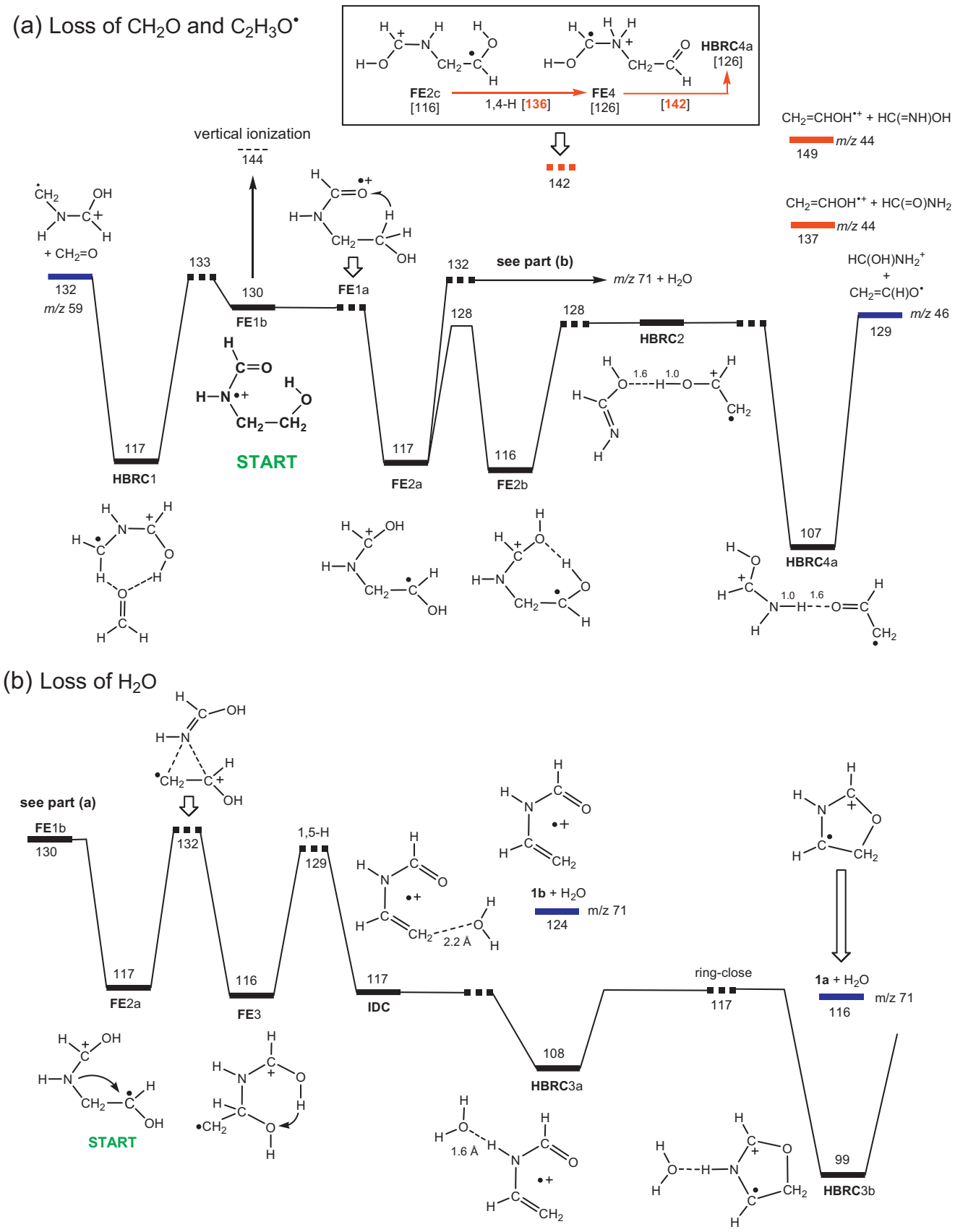

Scheme 7. Mechanistic proposals for the losses of CH_2O and CH_2=$CHO^{\bullet}$ (top), and H_2O (bottom) from *N*-formylethanolamine ions **FE**1. The numbers refer to 298 K enthalpies derived from CBS-QB3 calculations.

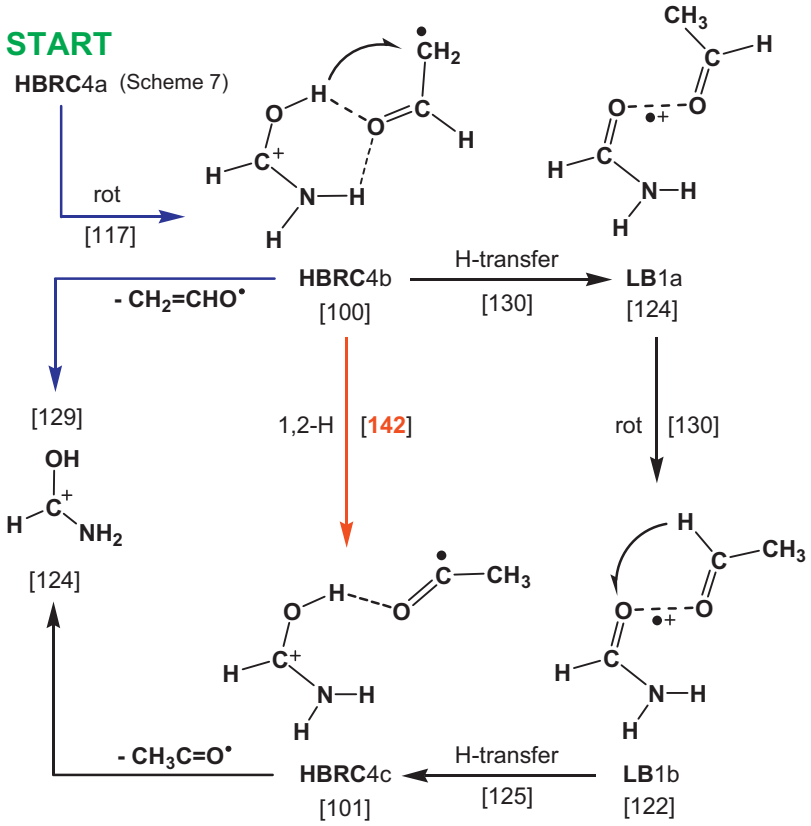

Scheme 8. The proposed quid-pro-quo catalysis mechanism that leads to the loss of $CH_3C{=}O^\bullet$ from ionized *N*-formylethanolamine. The numbers refer to 298 K enthalpies (in kcal mol^{-1}) derived from CBS-QB3 calculations.

Overall, the mechanism is characterized by the catalyst donating a proton to one site of the substrate, and subsequently abstracting a proton from a different site. This variant of proton-transport catalysis has been coined as quid-pro-quo catalysis [9b].

Returning to Scheme 7, it is seen in part (b) that the H_2O loss mechanism is initiated from distonic ion **FE**2a. Lengthening of its N–C bond leads to an ion–molecule complex of a vinyl alcohol ion and formimidic acid, which, at an energy level of 132 kcal mol^{-1}, may recombine to form distonic ion **FE**3. In essence, the reaction **FE**2 → **FE**3 involves transfer of the formimidic acid component of **FE**2 to the adjacent carbon in the vinyl alcohol moiety. A 1,5-H shift in **FE**3, followed by elongation of the incipient C–OH_2^+ bond, results in the formation of ion–dipole complex **IDC** at 117 kcal mol^{-1}. Ion **IDC** may either dissociate into the *N*-vinylformamide ion **1b** + H_2O, or adopt the configuration of **HBRC**3a at 108 kcal mol^{-1}.

As discussed in Section 3.1, solitary ions **1b** may cyclize to the more stable distonic ions **1a** and the same reaction may also occur in **HBRC**3a to produce **HBRC**3b, with the water molecule acting as a spectator. Since the associated TS lies well below the dissociation threshold **1b** + H_2O, a mixture of ions **1a** and **1b** may be generated. This is consistent with the analysis of the CID spectrum of the *m*/*z* 71 ions in Section 3.2.

Finally, we note that the mechanisms of Scheme 7 have no reverse barriers, in line with the observed modest $T_{0.5}$ values of 23, 18 and 36 meV for the formation of the *m*/*z* 46, 59 and 71 ions.

3.5. The dissociation behaviour of D- and ^{18}O-isotopologues of *N*-formylethanolamine

To seek further support for the proposals of Scheme 7, we have examined the MI mass spectra of the D- and ^{18}O-labelled molecular ions of Table 3. For the sake of clarity, the Table expresses the normalized MI peak intensities as neutral losses.

First we note that the proposals of Scheme 7 for the losses of CH_2O and $C_2H_3O^\bullet$ are entirely compatible with the labelling data of Table 3 as are the CID spectra of the labelled product ions (not shown). It is also obvious that D isotope effects are operating in these losses but, given the complexity of the system, these were not further analyzed.

In contrast, the data pertaining to the water loss suggest that a partial exchange of the H and O atoms occurs or that this reaction involves additional (minor) dissociation pathways.

The aldehydic hydrogen does not participate in the proposal of Scheme 7b and indeed ions $HOCH_2CH_2NHC\mathbf{D}O^{\bullet+}$ predominantly lose H_2O. However, ~25% of the ions lose HDO and mechanisms that could account for this observation are presented in Scheme 9.

One option is that ion **FE**3 of Scheme 7b undergoes a competing 1,5-H shift of the same TS-energy: the route **FE**3 → **FE7** → **1f** + HDO of Scheme 9. This proposal is not attractive, considering that the CID spectrum of the 3-methylaziridinone ion [21b], the cyclic isomer of distonic ion **1f**, is characterized by an intense CH_3 loss and that this loss is absent in the CID spectrum of Fig. 3c.

An intriguing alternative is the H/D exchange reaction depicted at the bottom of Scheme 9. Here, the H_2O molecule of **HBRC**3a abstracts the aldehydic *deuteron* and then donates a *proton* back to the carbonyl oxygen atom, yielding **HBRC**8 in a QPQ type reaction. Loss of HDO from **HBRC**8 is likely too energy demanding but TS **HBRC**3a → 8 may be sufficiently accessible (138 kcal mol^{-1}) to account for a partial exchange of the H_2O hydrogens and the aldehydic deuterium of ions **HBRC**3a by a back-and-forth QPQ reaction with **HBRC**8.

The minor loss of D_2O from $\mathbf{D}OCH_2CH_2N\mathbf{D}CHO^{\bullet+}$ may also arise from a QPQ type reaction: Scheme 9 shows that TS **HBRC**3a → 7 lies

Table 3
The neutral losses in the MI spectra of various isotopologues of *N*-formylethanolamine.

Ion	Neutral lost								
	$C_2H_3O^{\bullet}$	$C_2\mathbf{D_3}O^{\bullet}$	CH_2O	$C\mathbf{D_2}O$	H_2O	HDO	$H_2\mathbf{O}$	HDO	$\mathbf{D_2}O$
$HOCH_2CH_2NHCHO^{\bullet+}$	100	–	77	–	45	–	–	–	–
$HOCH_2CH_2NHC\mathbf{D}O^{\bullet+}$	100	–	92	–	38	13	–	–	–
$\mathbf{D}OCH_2CH_2N\mathbf{D}CHO^{\bullet+}$	100	–	53	–	5	40	–	–	10
$HOC\mathbf{D_2}C\mathbf{D_2}NHCHO^{\bullet+}$	–	100	–	47	13	23	–	–	–
$HOCH_2CH_2NHC\mathbf{O}^{\bullet+}$	100	–	80	–	40	–	10	–	–
$HOCH_2CH_2NHC\mathbf{DO}^{\bullet+}$	100	–	83	–	30	4	6	5	–

The 18-O and D isotopes are printed in bold face; intensities relative to the most intense loss = 100%.

so low in energy, at 118 kcal mol^{-1}, that the hydronium hydrogens of **HBRC**3a are expected to exchange prior to dissociation. Loss of D_2O may also occur from **HBRC**7 to generate **1c**, a tautomer of the *N*-vinylformamide ion. The minor H_2O loss from $\mathbf{D}OCH_2CH_2N\mathbf{D}CHO^{\bullet+}$ may similarly be explained by the QPQ transformation **HBRC**3a → 8 mentioned above. Finally, by invoking the above exchange reactions, the losses of HDO and H_2O from $HOC\mathbf{D}_2C\mathbf{D}_2NHCHO^{\bullet+}$ can also be rationalized.

Table 3 shows, in agreement with the mechanism of Scheme 7b, that most of the ions $HOCH_2CH_2NHCH^{18}O^{\bullet+}$ lose their hydroxyl oxygen as H_2O^{16}. However, ~25% of the ions loses the labelled amide oxygen. We further note that ions $HOCH_2CH_2NHC\mathbf{D}^{18}O^{\bullet+}$ lose H_2O, HDO, $H_2{}^{18}O$ and $HD^{18}O$, which indicates that the loss of the ^{18}O- and D-labels involves different (exchange) mechanisms.

A likely rationale for the partial loss of the ^{18}O-label is that a key intermediate of Scheme 7 communicates with an isomer whose oxygen atoms are equivalent. This scenario was probed by many exploratory calculations that yielded the two pathways depicted in Scheme 10 as plausible candidates. The first one involves ion **FE**9 generated by the route **IDC** → **FE**8 → **FE**9. In this reaction, the water molecule of **IDC** attacks the terminal methylene group and synchronously transfers one of its hydrogens to the carbonyl oxygen atom. The resulting ion **FE**8 may then undergo a 1,4-OH shift to generate ion **FE**9. The second option is slightly more energy

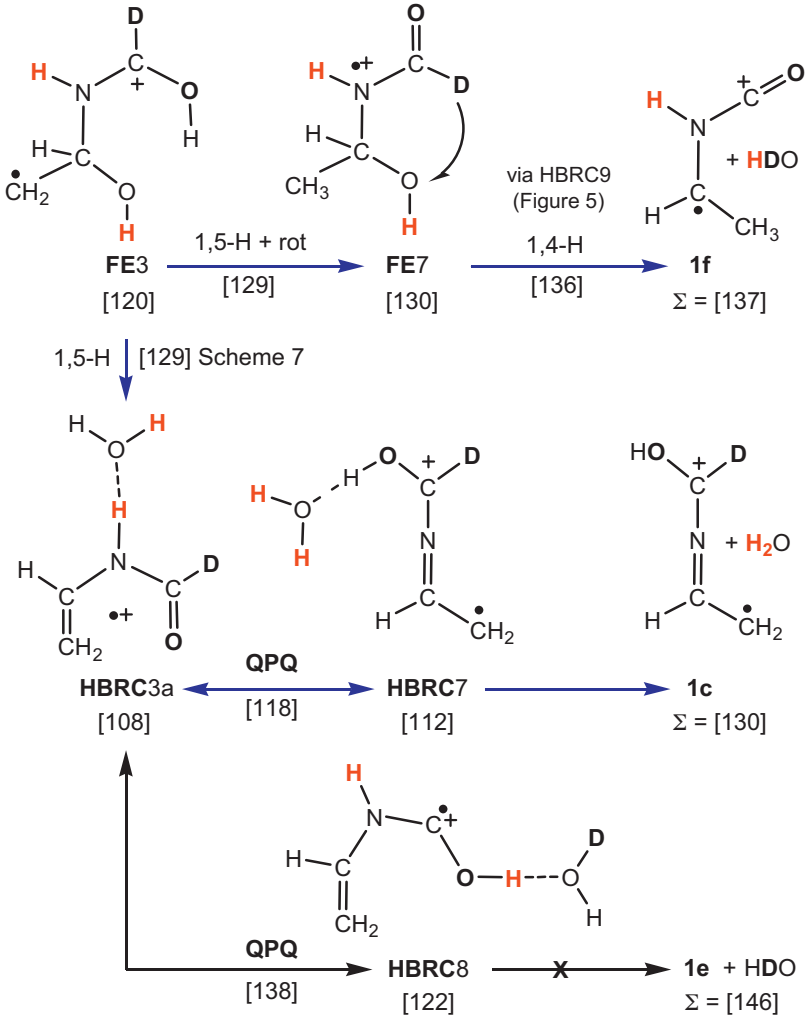

Scheme 9. Potential pathways for the minor HDO loss from the *N*-formylethanolamine isotopologue $HOCH_2CH_2NHCDO$. Numbers in brackets are CBS-QB3 derived 298 K enthalpies in kcal mol^{-1}.

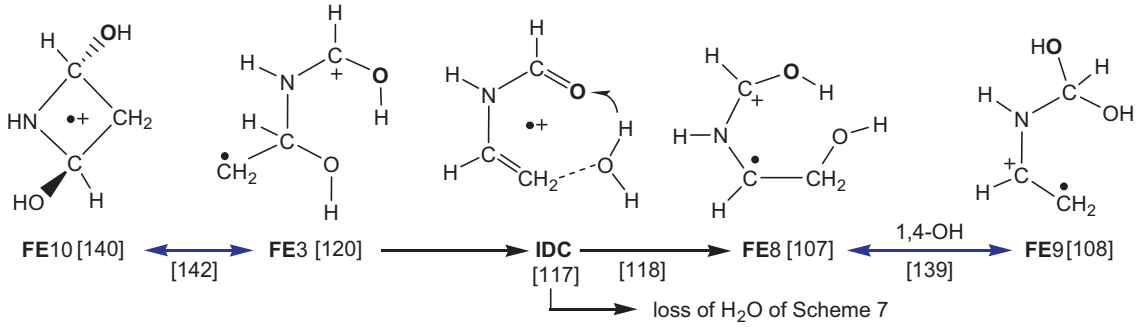

Scheme 10.

demanding: it involves cyclization of ion **FE**3 to the symmetric ion **FE**10.

The energy of the TS of these exchange routes lies below that of the incipient molecular ions **FE**1 of Scheme 7 (144 kcal mol^{-1}), but well above the dissociation threshold **1** + H_2O. This may be the reason why only a fraction of the ^{18}O-labelled ions loses the positional identity of the oxygen atoms prior to dissociation. In the same vein, the proposed H/D exchange reactions of the D-labelled ions do not lead to a statistical distribution of the label [28].

3.6. The losses of H_2O and CO from protonated *N*-formylethanolamine

N-formylethanolamine may be protonated at three different sites: at the amide oxygen, the amide nitrogen, or the hydroxyl oxygen. The resulting ions, **PFE**1a–c, are shown in Scheme 11. As expected, the carbonyl protonated ion **PFE**1a is calculated to have a much greater stability than the other tautomers.

Tip et al. [14] propose that the prominent loss of H_2O (see Fig. 2c and d) is initiated by a 1,3-H shift in *N*-protonated ions **PFE**1b, yielding *N*-protonated *N*-vinylformamide. This, however, is at odds with our observation that D-labelled ions $DOCH_2CH_2NDCHOD^+$ specifically lose D_2O. Moreover, the proposed 1,3-H shift is undoubtedly quite energy demanding, much like the 1,3-H shift connecting **PFE**1a and **PFE**1b in Scheme 11.

Instead, we propose that the water loss involves a concerted cyclization and direct bond cleavage in **PFE**1c. The resulting proton-bridged ion **PFE**2 may then lose water (as D_2O) to produce protonated *2*-oxazoline. An analogous mechanism has been proposed for the loss of H_2O from serine residues in protonated peptides and proteins [29].

A direct 1,2-H shift in **PFE**1b [14] cannot account for the competing loss of CO because it requires 24 kcal mol^{-1} more energy than our proposed H_2O loss mechanism. However, a search of the potential energy surface yielded the remarkable structure "TS [95]" of Scheme 11, whose energy lies 2 kcal mol^{-1} below the rate-determining TS for the water loss. In this decarbonylation, the amide N–C bond of "TS [95]" elongates as the aldehydic H is transferred to the hydroxyl group. The resulting transient complex, comprising the *O*-protonated species $NH_2CH_2CH_2OH_2^+$ and CO, then rearranges via a 1,4-H shift to produce $^+NH_3CH_2CH_2OH$ + CO.

As suggested in Section 3.1, the notable peaks at *m*/*z* 71, 59 and 46 in the CID spectrum of PFE ions generated by self-protonation (Fig. 2d) arise from **PFE** ions that have lost a H$^\bullet$ radical to produce *m*/*z* 89 ions having dissociation characteristics akin to those of ionized *N*-formylethanolamine. We have not computationally examined the myriad of NFEA isomers that can be envisaged to be generated upon H$^\bullet$ loss. An attractive possibility is that distonic ion **FE**2 of Scheme 7, a key intermediate in the dissociation of ion **FE**1, is generated.

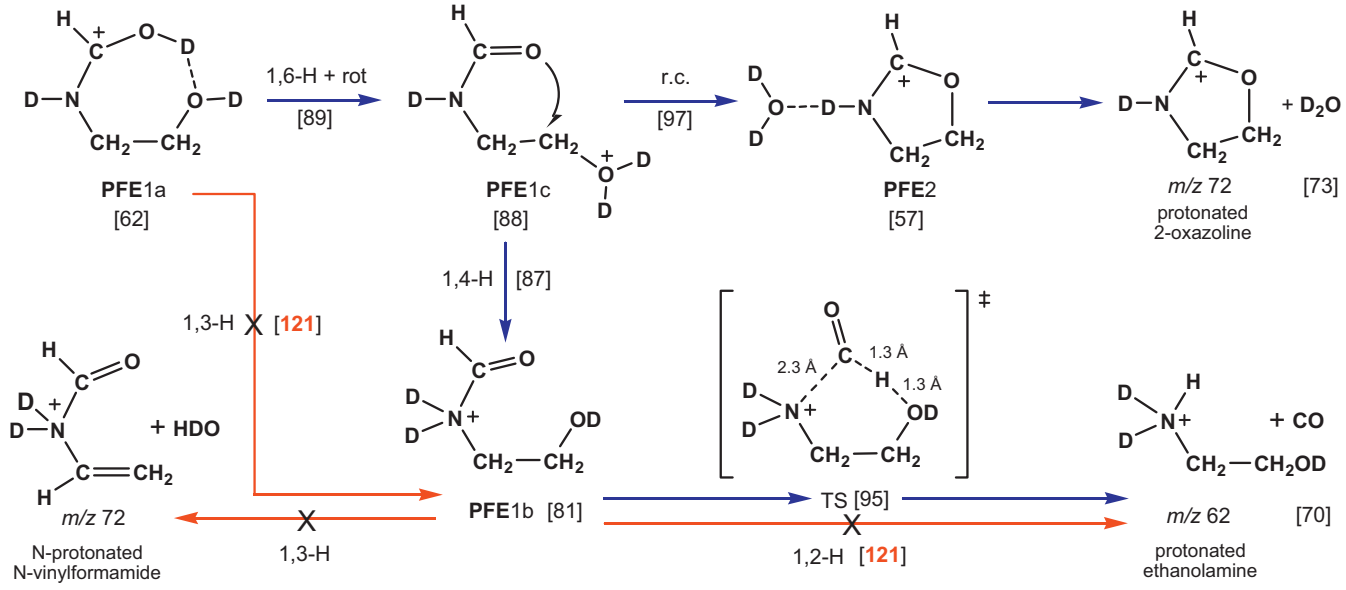

Scheme 11. Mechanistic proposals for the losses of H_2O and CO from protonated *N*-formylethanolamine (**PFE**1a). Numbers in brackets are CBS-QB3 derived 298 K enthalpies in kcal mol^{-1}.

4. Summary

The fruitful interplay of theory and experiment of this study reveals that distonic ions and hydrogen-bridged radical cations (HBRCs) play a key role in the fascinating dissociation chemistry of the *N*-formylethanolamine radical cation, $HOCH_2CH_2NHC(H)=O^{\bullet+}$ (**FE**1).

As discussed in Section 3.2, the primary fragmentations involving the loss of CH_2O and $C_2H_3O^{\bullet}$ yield the distonic ion $^{\bullet}CH_2N(H)CHOH^+$ and *O*-protonated formamide $HC(OH)NH_2^+$ respectively. The competing H_2O loss yields a mixture of *N*-vinylformamide ions **1b** and its cyclized distonic isomer **1a**: the CID spectrum is very close to a reference spectrum of **1b**, but its enhanced charge-stripping peak betrays that ions **1a** are also present.

Rotation of the amide C–N bond of neutral and ionized *N*-formylethanolamine involves a sizeable energy barrier. In Section 3.3 and Scheme 6, theory provides a rationale for the experimental finding that the ions do not decarbonylate which implies that these geometrical isomers have the same dissociation characteristics.

The mechanistic analysis of Section 3.4 and Scheme 7 indicates that:

(i) cleavage of the C–C bond in the incipient molecular ions **FE**1 generates **HBRC**1, $[CH_2N(H)C(H)=O\cdots H\cdots O=CH_2]^{\bullet+}$, which serves as the direct precursor to CH_2O loss.

(ii) a competing 1,5-H shift, the first step of a McLafferty rearrangement, generates distonic ion **FE**2, $HOCHCH_2N(H)C(H)OH^{\bullet+}$,which serves as the precursor for the loss of both $C_2H_3O^{\bullet}$ and H_2O.

(iii) loss of $C_2H_3O^{\bullet}$ from **FE**2 involves a "McLafferty + 1″ type reaction in which HBRCs act as key intermediates: **FE**2 → **HBRC**2 → **HBRC**4a → $HC(OH)NH_2^+ + CH_2=CHO^{\bullet}$. Prior to dissociation, a fraction of ions **HBRC**4a may undergo the quid-pro-quo (QPQ) catalysis of Scheme 8, which would co-generate the more stable acetyl radical $CH_3C=O^{\bullet}$.

(iv) loss of H_2O from **FE**2 involves communication with ion–molecule complexes of vinyl alcohol and formimidic acid, whose components may recombine to form distonic ion **FE**3, $HOCH(CH_2)N(H)C(H)OH^{\bullet+}$. This ion loses H_2O via the 1,5-H shift reaction **FE**3 → **HBRC**3a → ion **1b** + H_2O. The facile cyclization of **HBRC**3a to **HBRC**3c may account for the co-generation of ion **1a**.

The behaviour of the various D- and ^{18}O-labelled isotopologues examined in Section 3.5 is basically in accord with the above mechanisms. The MI spectra of the labelled ions indicate that, in the loss of water, the positional identity of the D and O atoms is not completely retained. A rationale provided by theory for this finding involves the participation of the QPQ type reactions of Scheme 9 for H/D exchange. Scheme 10 presents two side reactions of ion **IDC**, a key intermediate in the H_2O loss of Scheme 7, that lead to unreactive isomers whose O atoms are equivalent. These reactions could account for the partial equilibration of the O-atoms.

Finally, a re-examination of the dissociation of protonated *N*-formylethanolamine proposes that the losses of H_2O and CO generate protonated *2*-oxazoline and *N*-protonated ethanol-amine respectively via the mechanisms of Scheme 11.

Acknowledgements

The role of the late Professor Dudley Williams in developing and popularising experimental approaches to studying and describing the reactions of ions [30], his enthusiasm for science, and his influence on scientists of many persuasions and interests, is acknowledged with thanks

JKT and KJJ thank the Natural Sciences and Engineering Research Council of Canada (NSERC) for financial support and Prof. N.H. Werstiuk for obtaining the UV photoelectron spectrum of *N*-formylethanolamine. The assistance of Mr Tariq Mahmood in optimising conditions for the condensation of ethanolamine with methyl formate is gratefully acknowledged.

References

[1] (a) I. Howe, D.H. Williams, R.D. Bowen, Mass Spectrometry: Principles and Applications, second ed., McGraw-Hill International Book Company, New York, 1981;
(b) F.W. McLafferty, F. Tureček, Interpretation of Mass Spectra, fourth ed., University Science Books, Mill Valley, 1993, p. 81;
(c) R.M. Smith, Understanding Mass Spectra: A Basic Approach, second ed., John Wiley & Sons, Hoboken, 2004, p. 234;
(d) F. Tureček, in: N.M.M. Nibbering (Ed.), Encyclopedia of Mass Spectrometry, vol. 4, Elsevier, Amsterdam, 2005, p. 396.
[2] M.B. Stringer, D.J. Underwood, J.H. Bowie, C.E. Allison, K.F. Donchi, P.J. Derrick, Org. Mass Spectrom. 27 (1992) 270.
[3] D. Kuck, in: N.M.M. Nibbering (Ed.), Encyclopedia of Mass Spectrometry, vol. 4, Elsevier, Amsterdam, 2005, pp. 110–111.
[4] (a) G. Bouchoux, Y. Hoppilliard, Int. J. Mass Spectrom. 90 (1989) 197;
(b) C.E. Hudson, L.L. Griffin, D.J. McAdoo, Org. Mass Spectrom. 24 (1989) 866;
(c) A.E. Dorigo, M.A. McCarrick, R.J. Loncharich, K.N. Houk, J. Am. Chem. Soc. 112 (1990) 7508.
[5] (a) J. Loos, D. Schröder, W. Zummack, H. Schwarz, R. Thissen, O. Dutuit, Int. J. Mass Spectrom. 214 (2002) 105;
(b) M. Semialjac, J. Loos, D. Schröder, H. Schwarz, Int. J. Mass Spectrom. 214 (2002) 129;
(c) D. Schröder, J. Loos, M. Semialjac, T. Weiske, H. Schwarz, G. Hohne, R. Thissen, O. Dutuit, Int. J. Mass Spectrom. 214 (2002) 155.
[6] (a) J.A. Montgomery Jr., M.J. Frisch, J.W. Ochterski, G.A. Petersson, J. Chem. Phys. 112 (2000) 6532;
(b) L.A. Curtiss, P.C. Redfern, K. Raghavachari, J. Chem. Phys. 126 (2007) 084108;
(c) J.M.L. Martin, S. Parthiban, in: J. Cioslowski, A. Szarecka (Eds.), Quantum Mechanical Prediction of Thermochemical Data, Understanding Chemical Reactivity Series, vol. 22, Kluwer Academic Publishers, Dordrecht, 2005, pp. 31–65;
(d) L.N. Heydorn, Y. Ling, G. de Oliveria, J.M.L. Martin, Ch. Lifshitz, J.K. Terlouw, Z. Phys. Chem. 215 (2001) 141.
[7] (a) R. Lee, P.J.A. Ruttink, P.C. Burgers, J.K. Terlouw, Can. J. Chem. 83 (2005) 1847;
(b) K.J. Jobst, T.R. Khan, J.K. Terlouw, Int. J. Mass Spectrom. 42 (2007) 1024.
[8] P.C. Burgers, J.K. Terlouw, in: N.M.M. Nibbering (Ed.), Encyclopedia of Mass Spectrometry, vol. 4, Elsevier, Amsterdam, 2005, p. 173.
[9] (a) R. Lee, P.J.A. Ruttink, P.C. Burgers, J.K. Terlouw, Int. J. Mass Spectrom. 255 (2006) 244, and references cited therein;
(b) K.J. Jobst, P.C. Burgers, P.J.A. Ruttink, J.K. Terlouw, Int. J. Mass Spectrom. 254 (2006) 127.
[10] (a) D.J. McAdoo, C.E. Hudson, M. Skyiepal, E. Broido, L.L. Griffin, J. Am. Chem. Soc. 109 (1987) 7648;
(b) J. Loos, D. Schröder, H. Schwarz, J. Org. Chem. 70 (2005) 1073.
[11] J.L. Holmes, K.J. Jobst, J.K. Terlouw, J. Labelled Compd. Radiopharm. 50 (2007) 1088.
[12] (a) H.F. van Garderen, P.J.A. Ruttink, P.C. Burgers, G.A. McGibbon, J.K. Terlouw, Int. J. Mass Spectrom. Ion Process. 121 (1992) 159;
(b) N.H. Werstiuk, D.N. Butler, E. Shahid, Can. J. Chem. 65 (1986) 760.
[13] J.L. Holmes, C. Aubry, P.M. Mayer, Assigning Structures to Ions in Mass Spectrometry, CRC Press, Boca Raton, 2007.
[14] L. Tip, C. Versluis, J.W. Dallinga, W. Heerma, Anal. Chim. Acta 241 (1990) 219.
[15] M.J. Frisch et al. Gaussian 03 (Revision C.02), Gaussian, Inc., Wallingford CT, 2004.
[16] G. Schaftenaar, R. Postma, P.J.A. Ruttink, P.C. Burgers, G.A. McGibbon, J.K. Terlouw, Int. J. Mass Spectrom. Ion Process. 100 (1990) 521.
[17] G.A. McGibbon, P.C. Burgers, J.K. Terlouw, Int. J. Mass Spectrom. 136 (1994) 191.
[18] P.R. Schreiner, H.P. Reisenauer, F.C.I.V. Pickard, A.C. Simmonett, W.D. Allen, E. Matyus, A.G. Csaszar, Nature 453 (2008) 906.
[19] (a) G. da Silva, C.-H. Kim, J.W. Bozzelli, J. Phys. Chem. A 110 (2006) 7925;
(b) E.A. Fogleman, H. Koizumi, J.P. Kercher, B. Sztáray, T. Baer, J. Phys. Chem. A 108 (2004) 5288;
(c) G. Bouchoux, J. Chamot-Rooke, D. Leblanc, P. Morgues, M. Sablier, Chem. Phys. Chem. 2 (2001) 235.
[20] B.L.M. van Baar, P.C. Burgers, J.L. Holmes, J.K. Terlouw, Org. Mass Spectrom. 23 (1988) 355 (note that the CIDI mass spectra of $CH_3CO^{\bullet}$ (Fig. 2a) and $CH_2CHO^{\bullet}$ (Fig. 2b) are transposed).
[21] (a) T. Wong, J. Warkentin, J.K. Terlouw, Int. J. Mass Spectrom. Ion Process. 115 (1992) 33;
(b) M.M. Cordero, J.J. Houser, C. Wesdemiotis, Anal. Chem. 65 (1993) 1594.
[22] J.K. Terlouw, P.C. Burgers, H. Hommes, Org. Mass Spectrom. 14 (1979) 387.
[23] P.J.A. Ruttink, P.C. Burgers, J.K. Terlouw, Int. J. Mass Spectrom. Ion Process. 145 (1995) 35.

[24] (a) D.M. Pawar, A.A. Khalil, D.R. Hooks, K. Collins, T. Elliot, J. Stafford, L. Smith, E.A. Noe, J. Am. Chem. Soc. 120 (1998) 2108;
(b) J.P. Terhorst, W.L. Jorgensen, J. Chem. Theory Comput. 6 (2010) 2762.
[25] W. Heerma, M.M. Sarneel, J.K. Terlouw, Org. Mass Spectrom. 16 (1981) 326.
[26] S. Nakajima, T. Asakawa, O. Sekiguchi, S. Tajima, N.M.M. Nibbering, Eur. J. Mass Spectrom. 7 (2001) 47.
[27] (a) P.M.W. Gill, L. Radom, J. Am. Chem. Soc. 110 (1988) 4931;
(b) S. Humbel, I. Côte, N. Hoffmann, J. Bouquant, J. Am. Chem. Soc. 121 (1999) 5507.
[28] R.G. Cooks, J.H. Beynon, R.M. Caprioli, G.R. Lester, Metastable Ions, Elsevier Scientific Publishing Company, New York, 1973, p. 257.
[29] B. Paizs, S. Suhai, Mass Spectrom. Rev. 24 (2005) 508.
[30] (a) D.H. Williams, Acc. Chem. Res. 10 (1977) 280;
(b) R.D. Bowen, D.H. Williams, H. Schwarz, Angew. Chem. Int. Ed. Eng. 18 (1979) 451.